



*The 19th International Conference on
Global Research and Education
In Engineering for Sustainable Future*

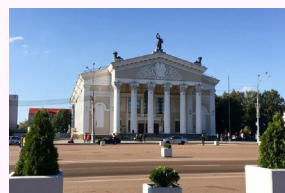
inter-Academia 2021

20 – 22 October, 2021

Gomel, BELARUS

**Venue: Francisk Skorina Gomel State University
104 Sovetskaya str., Gomel, Belarus**

PROGRAM AND BOOK OF ABSTRACTS



GENERAL CHAIRS

Igor V. Semchenko, Oleg M. Demidenko, Alexander V. Rogachev

HONORARY COMMITTEE

Host Rector

Sergei A. Khakhomov,

Francisk Skorina Gomel State University, Belarus

and Rectors

Kazuyuki Hizume, Shizuoka University

Marek Stevcek, Comenius University, Slovakia

János Józsa, Budapest University of Technology and Economics, Hungary

Krzysztof Zaremba, Warsaw University of Technology, Poland

Lambert T. Koch, Wuppertal University, Germany

Tudorel Toader, Alexandru Ioan Cuza University, Romania

Leonids Ribickis, Riga Technical University, Latvia

Martin Bares, Masaryk University, Czech Republic

Anastas Gerdjikov, Sofia University, Bulgaria

Levente Kovacs, Óbuda University, Hungary

Volodymyr A. Buhrov, Taras Shevchenko National University of Kyiv, Ukraine

Andrey P. Shevchik, St. Petersburg State Technological Institute, Russia

Eugenijus Valatka, Kaunas University of Technology, Lithuania

Igor Sarov, Moldova State University, Moldova

INTERNATIONAL ADVISORY CONFERENCE COMMITTEE

Annamária R. Várkonyi-Kóczy (Óbuda University, Hungary)

Arturs Medvids (Riga Technical University, Latvia)

Gheorghe Popa (Prof. Emeritus, Alexandru Ioan Cuza University, Romania)

Evgenia Benova (Sofia University, Bulgaria)

Dumitru Luca (Prof. Emeritus, Alexandru Ioan Cuza University, Romania)

Hidenori Mimura (Shizuoka University, Japan)

Hiroshi Mizuta (University of Southampton, England)

Kenji Murakami (Shizuoka University, Japan)

Leonid Poperenko (Taras Shevchenko National University of Kyiv, Ukraine)

Lucel Sirghi (Alexandru Ioan Cuza University, Romania)

Masaaki Nagatsu (Prof. Emeritus, Shizuoka University, Japan)

Masashi Kando (Prof. Emeritus, Shizuoka University, Japan)

Michiharu Tabe (Prof. Emeritus, Shizuoka University, Japan)

Kazuhiko Hara (Shizuoka University, Japan)

Nobuyuki Araki (Prof. Emeritus, Shizuoka University, Japan)

Noriko Matsuda (Shizuoka University, Japan)

Nicoleta Dumitrascu (Alexandru Ioan Cuza University, Romania)

Ryszard Jablonski (Warsaw University of Technology, Poland)

Jan Maciej Kościelny (Warsaw University of Technology, Poland)

Małgorzata Kujawińska (Warsaw University of Technology, Poland)

Sergiusz Łuczak (Warsaw University of Technology, Poland)

Roman Szewczyk (Warsaw University of Technology, Poland)

Adam Woźniak (Warsaw University of Technology, Poland)

Sergei Khakhomov (Gomel State University, Belarus)

Stefan Matejčík (Comenius University, Slovakia)

Valdis Kokars (Riga Technical University, Latvia)

Giedrius Laukaitis (Kaunas University of Technology, Lithuania)

Maxim M Sychov (Saint Petersburg State Institute of Technology, Russia)

Volodymyr Gnatyuk (National Academy of Sciences of Ukraine)

Yoshimasa Kawata (Shizuoka University, Japan)

Jun Kondoh (Shizuoka University, Japan)

LOCAL ORGANIZING COMMITTEE

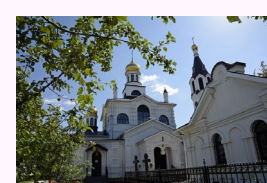
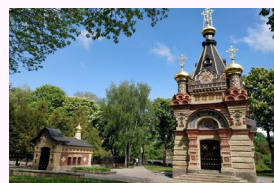
Dmitry Kovalenko, Francisk Skorina Gomel State University, Belarus

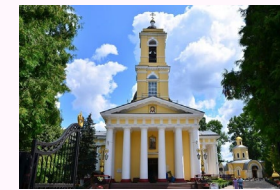
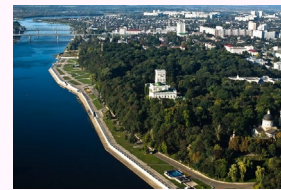
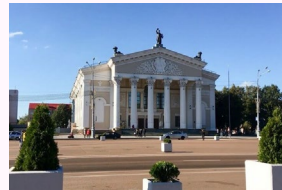
Andrey Samafalov, Francisk Skorina Gomel State University, Belarus

Andrey Sereda, Francisk Skorina Gomel State University, Belarus

Oksana Deruzhkova, Francisk Skorina Gomel State University, Belarus

Tatyana Lozovskaya, Francisk Skorina Gomel State University, Belarus



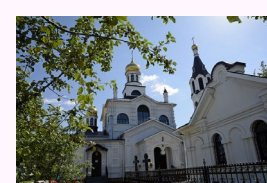
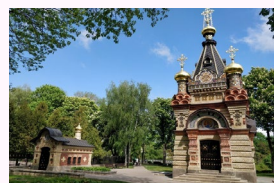


CONFERENCE FOCUS

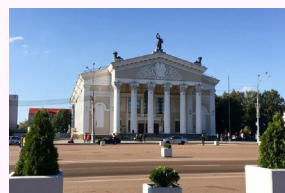
The International Conference on Global Research and Education, Inter-Academia 2021 is the continuation of the thriving event series organized by the Inter-Academia community every autumn since 2002. These conferences serve as foot-stones of the international scientific network promoting Inter-Academia philosophy and the academic and social interactions among professors, researchers, and students of the leading Shizuoka University (Japan) and that of the European member universities from Central and Eastern Europe.

CONFERENCE TOPICS

- [Bio- and environmental engineering](#)
- [Electric and Electronic engineering](#)
- [Intelligent and soft computing techniques](#)
- [Internet based education, distance learning](#)
- [Manufacturing technology](#)
- [Material science and technology, smart materials](#)
- [Measurement, identification, and control](#)
- [Metamaterials and metasurfaces](#)
- [Modeling and diagnostics](#)
- [Multimedia and E-learning techniques and materials](#)
- [Nanotechnology and nanometrology](#)
- [Photonics](#)
- [Plasma physics](#)



[illegible]



Author index

Aarthy M.
Abdilalizadeh L.
Agabekov V. Ye.
Airinei A.
Aksionova N.
Alagar Nedunchezian A. S.
Aleshkevich N. A.
Andrieieva O. L.
Aoki T.
Apetrei R. P.
Archana J.
Ardabili S.
Arivanandhan M.
Armetta F.
Arsentev M. Yu.
Asadchy V. S.
Athithya S.
Aushev I. Y.
Avdeeva E. V.
Ayvazyan G. Y.
Azhagar A.
Bakhmetev V. V.
Balabanov S. V.
Balmakou A.
Bayevich G. A.
Becker M.
Bekarevich R.
Berger M.
Besleaga A.
Bîrleanu E.
Blajan M. G.
Bogdanov S. P.
Borcia C.
Borcia G.
Buzhan A. V.
Calistru A. E.
Caponetti E.
Chekurvaev A. G.
Chirco G.
Ciaramitaro V.
Ciobanu A.

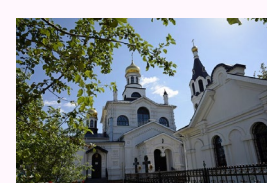
Ciolan M. A.
Costin C.
Creanga D.
Danilchenko K. D.
Dobromir M.
Dolgin A. S.
Dorokhina A. M.
Dovydenko E. M.
Emelyanov V. A.
Faniaveu I. A.
Fanyaev I. A.
Fedosenko N. N.
Fedosenko-Becker T. N.
Fesenko O.
Filippov V. V.
Filippovich L. V.
Firmansyah T.
Gaishun V. E.
Gnatyuk V. A.
Gomidze N. Kh.
Grishechkin Yu. A.
Grishechkina A. A.
Hakhoyan L. A.
Hara K.
Harish S.
Hashimoto K.
Hashimoto M.
Hatescu I.
Hayakawa K.
Hayakawa Y.
Hiroto T.
Hitomi K.
Honda T.
Hreniak D.
Ignatenko O. V.
Ignatovich J. V.
Ikeda H.
Ishiguro K.
Iwatsuki Y.
Javavel R.
Jialin Fang

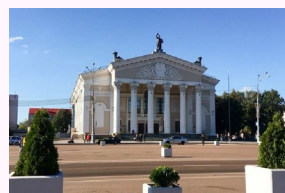
Jiang X.-H.
Jinxing Cao
Jitareanu G.
Kalaarasan K.
Kapshai V. N.
Kase H.
Kashko I. A.
Kawauchi T.
Keskinova M. V.
Khajishvili M. R.
Khakhomov S.
Kiselev D. A.
Kobayashi R.
Koike A.
Kominami H.
Kondoh J.
Konrad-Soare C. T.
Kontsevaya I. I.
Kosenok Ya. A.
Koshevaya K. S.
Košťál I.
Kovalenko D. L.
Koyama C.
Kravchenko A.
Kravets V. A.
Kristof J.
Kulesh E. A.
Kulyk O. P.
Kuznetsov P. A.
Laznev K. V.
Leibgam V.
Les A.
Lo Re G.
Luca D.
Luca M.
Makogon A. I.
Malvutina-Bronskaya V. V.
Matsui M.
Matsushita Y.
Maximenko A. V.
Masuzawa T.

Midiri M.
Mihaila I.
Mimura H.
Miron L. D.
Mitsuyoshi R.
Miyake T.
Molokanov A.
Moraru D.
Morii H.
Mosavi A.
Moskvichyov M. I.
Motrescu I.
Myshkovets V. N.
Nakagawa H.
Nakano T.
Navaneethan M.
Neo Y.
Nikiforov D. I.
Nikitjuk Yu. V.
Nishikawa K.
Nogami M.
Novik H. A.
Ohtake G.
Oishi R.
Okuyama T.
Onuma T.
Ota S. R.
Pandy C.
Paulenko A. V.
Petkevich A. V.
Pihosh Y.
Pilipenko V. A.
Piliptsov D. G.
Pobiyaha A. S.
Podshvvalova O. V.
Prokhorenko V. A.
Rahardjo E. T.
Rajasekaran P.
Rakos B.
Razmara J.
Rituraj R.

Rogachev A. A.
Rogachev A. V.
Rudnikov A. S.
Sakai H.
Sakai K.
Sakata H.
Saladino M. L.
Samofalov A.
Semchenko A. V.
Semchenko I.
Serdyukov A. N.
Sereda A. A.
Shainidze J. J.
Shalini V.
Shalupaev S. V.
Shamyna A. A.
Sharma P.
Shepelina A. Yu.
Shershnev E. B.
Shimizu K.
Shimomura M.
Shizuka H.
Shubbar M.
Shumskaya A. E.
Shvidkiy S.
Sidharth D.
Sidski V. V.
Singh Rohitkumar
Shailendra
Sirghi L.
Slepiankou D.
Sokolov S. I.
Soroka S. A.
Stoian G.
Sychov M. M.
Sysoev E. I.
Tabata K.
Tabe M.
Tabrizchi H.
Takagi K.
Takagi T.

Takeya K.
Talkachov A. I.
Tamura Y.
Tanaka Y.
Teodoroff-Onesim S.
Terao T.
Tifui G.
Timoshenko M. V.
Tkachenko V. I.
Tkachenko V. V.
Topala I.
Tóth T. J.
Tovoda K.
Tripathi S. R.
Tsebriienko T.
Tuchkovskii A. K.
Tusor B.
Tyulenkova O. I.
Uchida H.
Uesugi K.
Várkonyi Kóczy A. R.
Vaskevich V. V.
Vynogradova-Anik O.
Wibisono G.
Xiaohong Jiang
Yahava A. G.
Yamada R.
Yamada T.
Yamaguchi K.
Yamaguchi T.
Yaremkevych A.
Yarmolenko M. A.
Yiming Liu
Zalessky V. B.
Zelenska K.
Zelenska T.
Zhidko T. V.





Section "Bio- and environmental engineering"

Report 1: Investigating urban sustainability by emphasizing on the approaches for reducing fuel consumption using intelligent transportation system (*Leila Abdilalizadeh, Sina Ardabili, Amir Mosavi, Annamária R. Várkonyi Kóczy*)

Abstract. In the current situation, the city is regarded as a suitable place, and urbanization is the most desirable way of life. This tendency to urbanization has accelerated urban population growth, disproportionate urban expansion, and created environmental problems including increased pollution from transportation reduced fuel consumption, and, subsequently, reduced emissions of the most serious threats. Urban sustainable development, as a common way to reduce these adverse effects, can be effective by improving and enhancing the economic, social, and environmental conditions of the city. This can be achieved through multidisciplinary approaches by taking into account various aspects of ecological development such as safety, health, industrial metabolism, landscape, and awareness. Along with this important and necessary approach to reduce fuel consumption in the transportation field, which is the main objective of the present study, various approaches and methods have been proposed by researchers. But with the advent of ICT and intelligent transportation systems, these techniques and approaches have taken a new direction. Nowadays, solutions to reduce fuel consumption by using intelligent transportation systems have become one of the most popular areas of science. This study aims to evaluate the dimensions of urban ecology to attain the quality of a sustainable urban environment and provide suggestions for reducing the harmful effects on the environment by the transportation system.

Report 2: Environmental risk management by achieving sustainable development goals in architecture and urban engineering (*Leila Abdilalizadeh, Sina Ardabili, Amir Mosavi, Annamária R. Várkonyi Kóczy*)

Abstract. In today's world, the increasing progress of technology and urban construction has increased the variety of unknown hazards to the environment. This has led organizations to find a way to reduce these risks. In this regard, environmental risk assessment and sustainable development in architecture and urban engineering can be a good tool for achieving sustainable development goals. Risk Management is a new branch of management science that found its new place in a variety of trends including finance and capital, investment, trade, insurance, industrial, civil, military and safety projects, health and environmental management has found its place. Therefore, the purpose of the study is to review environmental risk management by introducing the performance of William Fine and PHA approaches in Environmental Risk Assessment and to achieve Sustainable development goals in architecture and urban engineering. It helps us to promote sustainable development in harmony with nature while reducing the level of environmental risks.

Report 3: The proton beam influence on the sensitivity of wheat plantlets to AgNP pollution-preliminary results (*A. Les, A.Molokanov, S. Shvidkiy, D. Creanga*)

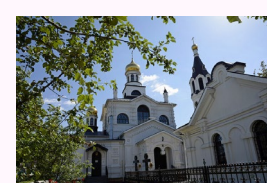
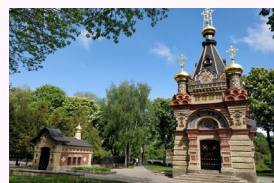
Abstract. Proton beam treatment of wheat seeds was carried out aiming to study the sensitivity of young plantlets that further have grown from seeds to environmental stress caused by nanoparticulate silver. The laboratory experiment evidenced diminished contents of assimilatory pigments in the lack of silver nanoparticles (AgNP) but higher values for diluted AgNP suspension.

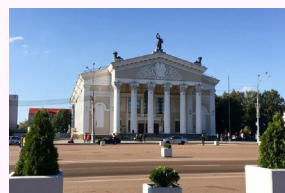
Report 4: Application of additive technology to create universal carriers of cellular structures (*E.M.Dovydenko, E.V.Avdeeva, K.V.Laznev, A.V.Petkevich, A.A.Rogachev, V.Ye.Agabekov*)

Abstract. In order to obtain biocompatible carriers with mechanical properties close to living tissues, 3D printing was performed with sodium alginate and chitosan hydrogels on a modified 3D printer based on the Wanhao Duplicator 4S (China) by installing a special extrusion head - a syringe extruder. The optimal compositions of sodium alginate and chitosan hydrogels for printing in a "supporting" agar and gelatin gel for fixing print objects have been determined. Optimal speeds of movement of the extruder-syringe for 3D printing with sodium alginate hydrogel into agar "supporting" gel 9–11 mm/s, for sodium alginate into gelatinous "supporting" gel - 2 mm/s, for chitosan into "supporting" gel with the addition of (NH₄)₂HPO₄–6–8 mm/s.

Report 5: Comparison and selection of the greenhouse gas accounting method for a model region in Germany (*T.N.Fedosenko-Becker, M.Becker, M.Berger*)

Abstract. Following the sustainable development trends, Germany is moving towards an energy transformation. This complex process requires serious planning and an interdisciplinary approach. Within the framework of the German project "WESTKUESTE100" the roadmaps to complete CO₂-neutrality in a model region will be offered. The first step to creating realistic scenarios is to analyze the existing accounting methods of greenhouse gas emissions and to adapt the chosen methods for the specific purposes. This work describes an approach to the selection and adaptation of a climate gas emission accounting method for a model region in order to create scenarios for the energy transformation.





Report 6: Evaluation of heavy metal contamination in mytilus sp. shells (I. Motrescu, M.A.Ciolan, A.E.Calistru, G.Jitareanu, L.D.Miron)

Abstract. Shellfish, such as Mytilus, are filter feeders, accumulating elements from the aquatic environment where they develop. Among these are heavy metal contaminants found in the water as a result of anthropogenic pollution. The mollusks are metabolizing these elements both into the consumable part and the crystalline structure of the shells, in different amounts, thus, these heavy metals being a possible threat for human consumption of shellfish. In this paper we use physical methods for the fast detection of heavy metals of some Mytilus sp. shells, and discuss the relevance and efficiency of these methods for bio-safety.

Report 7: In vivo measurement of dielectric properties of human skin using attenuated total reflection terahertz time domain spectroscopy (K.Hashimoto, H.Sakata, and S.R.Tripathi)

Abstract. The applications of terahertz (THz) waves have been increasing rapidly in different fields such as homeland security, non-destructive testing and next generation high speed communication. With the rapid development of such applications, encounters between THz waves and humans are expected to become common. Therefore, it is important to have the knowledge of terahertz properties of human skin in order to understand the interaction of terahertz wave with human skin. In this study, we developed attenuated total reflection terahertz time domain spectroscopy and measured the refractive index and absorption coefficient of skin in the frequency range of 200 GHz to 2 THz. This information help understand the terahertz wave interaction with human skin and other possible biomedical applications of terahertz wave such as assessment of skin hydration.

Report 8: Analysis of color coordinates in dried blood spots under aging for forensic medical applications (Kateryna Zelenska, Tetiana Zelenska, Olena Vynohradova-Anik, Toru Aoki)

Abstract. Color of a dried blood spot depends on the hemoglobin state and its amount in the aged spot. Digital images of the dried blood spots were analyzed in order to estimate color components depending on storage time. A level of chromaticity coordinate of g-component is almost stable while r- and b-components compete because of different contribution of hemoglobin states.

Section “Electric and Electronic engineering”

Report 9: Probing of deep states by band-to-band tunneling in nanoscale silicon-on-insulator Esaki diodes (D.Moraru, Y.Tamura, Y.Iwatsuki, K.Yamaguchi)

Abstract. Band-to-band tunneling (BTBT) is a fundamental transport mechanism that can be activated in highly-doped pn diodes, so-called Esaki diodes. In silicon, the indirect-bandgap nature poses some difficulties because phenomena such as phonon assistance are needed for momentum conservation purposes. In that sense, transport through deep, localized energy states in the depletion-layer can be of interest as an alternative to direct BTBT transport between the leads. Here, we present an analysis of silicon-on-insulator (SOI) Esaki diodes with nanoscale dimensions, in which excess current (at forward biases) contains current features that can be related to such deep states. The analysis covers also the role of a nanoscale i-layer inserted between the p+ and n+ leads in tuning the BTBT tunneling rate.

Report 10: A fluorescent protein-based AND gate for photon-coupled protein logic (Balázs Rakos)

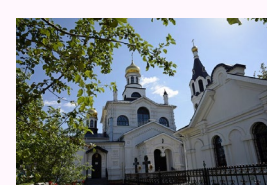
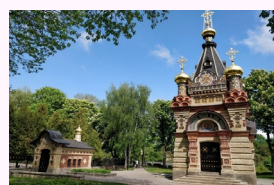
Abstract. We propose a fluorescent protein AND gate, which can serve as nanometer-scale building block in photon-coupled, protein-based logic circuits. The structure has numerous advantages with respect to previously introduced photoswitchable protein logic gates, such as its simplicity and faster response time. Furthermore, it can be accomplished with only a single molecule, and fluorescence is the sole requirement, which broadens the choices with respect to photoswitchable proteins. Besides its operational principle, readily available protein AND gates are introduced, and their integration into photon-coupled protein circuits is discussed, as well. We believe that the present work brings the realization of terahertz-speed molecular circuits yet another step closer.

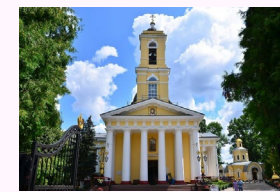
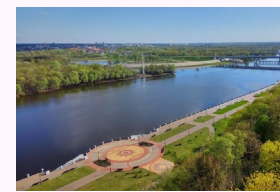
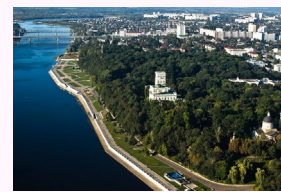
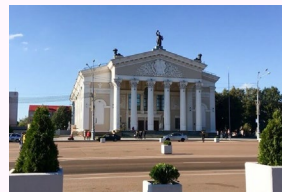
Report 11: An angle-sensitive, nickel bolometer-based, adaptive infrared pixel antenna (Mustafa Shubbar and Balázs Rakos)

Abstract. The present study proposes an infrared pixel antenna combined with readily-available, angle-sensitive, nickel bolometers. The antenna can automatically optimize itself for the direction of the incident mid-infrared radiation. The structure is expected to improve the performance of infrared sensors used in several areas, such as medicine, telecommunication and military. Furthermore, it can boost the efficiency of infrared energy harvesting applications, such as rectenna (antenna-rectifier) systems.

Report 12: Evaluation of radiation detection characteristics by α -Ga₂O₃ (H.Nakagawa, R.Yamada, M.Hashimoto, T.Yamaguchi, T.Onuma, T.Honda, T.Nakano, T.Aoki)

Abstract. In this study, we report on the radiation detection characteristics of α -Ga₂O₃ semiconductor radiation detector for evaluation possibility of radiation detection. The α -Ga₂O₃ sample was grown on c-plane sapphire substrate by mist chemical vapor deposition (mist-CVD) and the radiation detection characteristics were evaluated. The α -Ga₂O₃ detector exhibited good-sensitivity in the current-time change measurement with ²⁴¹Am α -particle irradiation. Moreover, the detection pulse signal of ²⁴¹Am α -particle was able to be obtained at room temperature. These results show α -Ga₂O₃ has the sensitivity of radiation and the possibility for application as room temperature radiation detector.





Report 13: Transportation and measurement of droplet using surface acoustic wave for digital microfluidic system application (Ryota Mitsuyoshi and Jun Kondoh)

Abstract. Nonlinear acoustic phenomena are caused by a surface acoustic wave (SAW) and a liquid. The principal is based on the radiated longitudinal wave from the SAW at the solid and liquid interface. Transportation and mixing are well-known phenomena. Those phenomena are important to realize a digital microfluidic system (DMFS) application. For the DMFS application, integration of a measurement function is necessary. In this paper, sound velocity was measured using the radiated longitudinal wave. The velocity measurements depend on the shape of the droplet. To keep the constant shape, slippery liquid-infused porous surface treatment was carried out. The improvement of the estimated velocity was confirmed with the treatment.

Report 14: 3D Fluorescence spectroscopy of liquid media via internal reference method (M.R.Khajishvili, N.Kh.Gomidze, J.J.Shainidze)

Abstract. Common methods of analyzing the chemical composition of a substance include many existing optical methods. Selecting an effective and optimal method from numerous optical methods and adapting it to the properties of the investigated substance is one of the most urgent tasks of modernity. Scientists are trying to study the substances – bioananoagents that surround humanity and develop methods and approaches that are used in one way or another to study the materials. The properties of materials are determined by considering both the main components and the compounds. In addition, often the properties of the materials depend on the distribution of the compounds or components in its volume.

Report 15: First-principles study of bandgap electronic states under electric field in silicon nanowires with discrete dopants (K.Yamaguchi, M.Tabe, D.Moraru)

Abstract. Low-dimensional Si tunnel diodes show a transport behavior significantly different compared to conventional (large-scale) devices due to dopant individuality. In this research work, we aim to understand the role of energy states which can be induced in the bandgap by the interaction between a donor-atom and an acceptor-atom in Si nanostructures. By means of ab initio (first-principles) simulations, we investigate the correlations between internal electric field, which is induced by the dopant atoms, and external electric field applied from outside. We find that high electric field makes the bandgap small because of a phenomenon equivalent to the Franz-Keldysh effect, even in such a small Si nanostructure. The effect is increased by the internal electric field which is induced by dopant atoms.

Report 16: High-performance and low-voltage current sense-amplifier using GAA-CNTFET with different chirality and channel (Singh Rohitkumar Shailendra, Pragya Sharma, M.Aarthy, Dr.Hidenori Mimura)

Abstract. This paper represents the Current sense amplifier based on GAA-Carbon nanotube field-effect transistor (CNTFET). Global demand for miniaturization of the device, researchers are struggling to design traditional transistors with less power and extraordinary speed. By far silicon transistors have been used but it reached its sub-10nm limit, beyond 10 nm it is suffering from many issues. To overcome these specific issues device designer reasonably concluded that CNTFET is a pronounced alternative by just doing little change in traditional silicon transistors. Parametric analysis has been efficiently performed on parameters like Power, Delay, and Power delay product by varying chirality vectors (n, m). Four unique configurations have been used as Single-channel single chirality (SCSC), double channel single chirality (DCSC), Single channel double chirality (SCDC), Double channel double chirality (DCDC). Based on the simulation result it is observed delay of the Current sense amplifier decreases with increased chirality and doubling the channel. Delay, Power, PDP analysis has been performed by varying t_{ox} and k_{ox} .

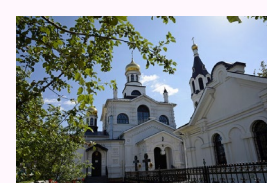
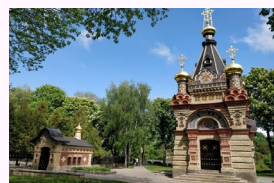
Report 17: Theoretical study of the impact of a donor-acceptor pair on tunneling current in Si nanodiodes (Chitra Pandey, K.Yamaguchi, Y.Neo, H.Mimura, M.Tabe, and D.Moraru)

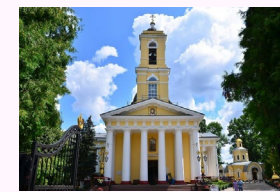
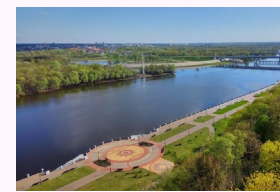
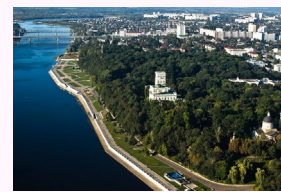
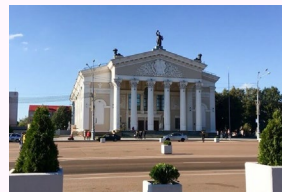
Abstract. Tunnel diodes are semiconductor devices that operate based on the band-to-band tunneling (BTBT) mechanism, a process that holds promise for future electronics. In Si, due to its indirect bandgap nature, the BTBT requires phonon assistance for momentum conservation. However, as device dimensions are reduced, discrete dopants at fronts of the depletion region can become critical in providing pathways for BTBT through localized or extended states. Here, we provide a theoretical study of the impact of a donor-acceptor pair on BTBT current, using a semi-empirical simulation approach. It is found that such a system can enhance the current and the main factors involved in this enhancement are identified distinctly.

Section “Intelligent and soft computing techniques”

Report 18: Intelligent pantry: a low cost smart storage manager for food spoilage prevention (B.Tusor, T.J.Tóth, A.R.Várkonyi-Kóczy)

Abstract. A home storage of various, perishable goods (e.g., food items, sanitary products, medical supplies etc.) is an integral part of any household. It gains even more importance in case of unexpected events such as pandemics, when people tend to stock up for months ahead. However, with higher amounts of perishable items, the probability of food spoilage (and thus, food waste) occurring is also higher, unless each item is carefully accounted for. In this paper, a novel smart storage framework is presented for tracking the expiration date and location of stored items and providing users with information and warnings about the goods in the storage, using cheap, affordable devices. Furthermore, the system can act as an advisor about replenishing supplies by learning the consumption habits and priorities of its users.





Report 19: A parallelization of instance methods of a .NET application that search for required structured data stored in a skip list (*I. Košťál*)

Abstract. The skip list is a more memory efficient version of a single level linked list. Searching for the required data elements in a skip list is more efficient than in a single level linked list because a skip list allows us to skip to the searched element in it. We have created a C# .NET application that uses a skip list with structured data in its data elements. This application can perform search operations within these data elements using serial, threaded, and parallelized instance methods, and simultaneously it is able to measure the execution times of particular methods. By comparing these times, we have examined the execution efficiency of parallelized instance methods of the object of the .NET application compared to threaded and serial instance methods of the same object. The results and evaluation of this examination are listed in the paper.

Report 20: Deep learning applications for COVID-19: a brief review (*Hamed Tabrizchi, Jafar Razmara, Amir Mosavi, A.R. Várkonyi-Kóczy*)

Abstract. Since December 2019, coronavirus disease (COVID-19) has affected most parts of human life. With the progression of time, COVID-19 was declared by the world health organization as an outbreak. Deep learning has been praised as one of the top methods in image-based healthcare applications. For this reason, a great number of research works have been proposed for the development of smart image-based diagnosis devices for the detection of COVID-19. This paper elaborates on summarizing the state-of-the-art research works related to deep learning applications for COVID-19 medical image processing to shed a light on the accelerated use of Deep Learning for COVID-19 research.

Report 21: Applications for effective representation of imaging with X-ray CT (*H.Kase, K.Takagi, K.Tabata, T.Aoki*)

Abstract. X-ray CT technology has currently advanced and provide high contrast and low noise imaging and material identification. Recent technology by AR (Augmented Reality) and VR (Virtual Reality) cannot represent large information by photon counting technology because it has intensity information and energy information. And, user couldn't observe internal structure and cross-section images. Two representing system that are by AR, and Spatial Reproduction Display with Motion capture has proposed. These systems organize information and allow users to observe the object at any angle intuitively and confirm the cross-sectional image. These problems have solved and could bring further innovations, such as coloring objects by composition.

Section "Internet based education, distance learning"

Report 22: The use of design automation tools in training young specialists in radio electronics (*A.A.Sereda, S.V.Shalupaev, Yu.V.Nikitjuk*)

Abstract. The paper considers the stages of mastering the computer-aided design of printed circuit boards for students of radio engineering specialties. The scheme allows a recent graduate to more effectively master the phases of constructing electronic devices and acquire professional skills in the development of printed wiring elements.

Section "Manufacturing technology"

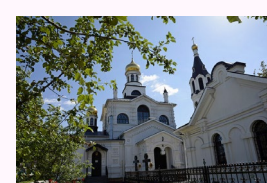
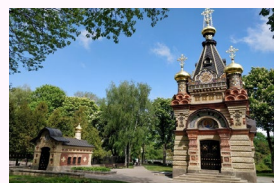
Report 23: Effects of process parameters on the dissimilar friction stir welded joints between aluminum alloy and polycarbonate (*A.Azhagar, K.Sakai, H.Shizuka, K.Hayakawa*)

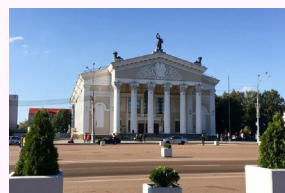
Abstract. Effects of processing parameters on weld interface and material flow during friction stir welding of dissimilar materials were investigated. The tapered cylindrical tool pin made of SKD11 was used to improve the in-process material flow behaviors during the process. In the experiments 3 mm thick plates of AA2017 aluminum alloy and polycarbonate were used as materials for welding at a tool rotation speed of 1320 or 1760 rpm, travel speed of 60mm/min, and tool offset of 2,3 or 4 mm toward AA2017. From the experiments, it was found the suitable process parameters for the butt welded joint, between the AA2017 and polycarbonate.

Section "Material science and technology, smart materials"

Report 24: Research of morphology and luminescence of particles based on yttrium fluorides for medical usage (*A.M.Dorokhina, H.Kominami, V.V.Bakhmetyev, Toru Aoki, Hisashi Morii*)

Abstract. The hydrothermal method is used to produce X-ray stimulated YF₃: Ce³⁺ nanophosphors with luminescence spectra and particle sizes suitable for photodynamic therapy. The influence of the synthesis media on the properties of particles is considered. The optimal duration of hydrothermal synthesis in an ethylene glycol medium has been revealed. The effect of various stabilizers (PEG, PVP, and PEI) on morphology and luminescent properties has been studied.





Report 25: One-step microwave synthesis of Eu^{2+} -doped silicate and chlorinesilicate phosphors mixture for application in light sources (*M.V.Keskinova, M.M.Sychov, K.Hara*)

Abstract. We have developed one-step microwave synthesis of Eu^{2+} -doped silicate and chlorinesilicate phosphors mixture, which can be used for light-sources application such as white-emitting diodes, luminiscent lamps and cathodoluminiscent white light sources. The mixture of phosphors $\text{Sr}_2\text{SiO}_4:\text{Eu}^{2+}$, $\text{CaSrSiO}_4:\text{Eu}^{2+}$, $\text{Ca}_{10}\text{Si}_6\text{O}_{21}\text{Cl}_2:\text{Eu}^{2+}$, $\text{Ca}_6\text{Sr}_4(\text{Si}_2\text{O}_7)_3\text{Cl}_2:\text{Eu}^{2+}$ has wide photoluminescence spectrum (around 150 nm) close to the sun-light, that provides high value of color rendering index (93) in the light source based on this phosphors mixture.

Report 26: Investigation of the convection effect on the inclusion motion in thermally stressed crystals (*O.P.Kulyk, V.I.Tkachenko, O.L.Andrieieva, O.V.Podshyvalova, V.A.Gnatyuk, T.Aoki*)

Abstract. The appearance and influence of convection in a liquid medium of inclusions on their motion in thermally stressed crystals is investigated taking into account the temperature gradient direction with regard to diffusion processes. Using the example of water-soluble alkaline-halide crystals, the values of Rayleigh and Prandtl numbers were estimated and the conditions of convective instability caused by the difference in temperature and solution concentration near the front and back surfaces of the inclusion were determined. It is shown that the contribution of convection to the processes of heat and mass transfer in a liquid medium of inclusions can result in a change in the kinetic laws of their motion in crystals.

Report 27: The role of the dispersed composition of the diamond matrix in the preparation of a composite by infiltration with molten silicon (*A.S.Dolgin, S.P.Bogdanov, V.Leibgam*)

Abstract. Diamond-silicon carbide composite is a new promising ceramic material with high hardness, strength, thermal conductivity and low density. The paper studies the effect of the dispersion of the diamond matrix of the composite on its properties.

Report 28: Digital Materials Science (*M.M.Sychov, A.G. Chekuryaev, S.P.Bogdanov, P.A.Kuznetsov*)

Abstract. "Industry 4.0" (4th industrial revolution) - the concept of digital production, all stages of the product life cycle are carried out on the basis of digital technologies. It should be supported by Digital Materials Science.

Report 29: Structure and properties of metal-carbon a-C coatings alloyed with Ti, Zr and Al with a high concentration (*Jialin Fang, D.G.Piliptsov, A.V.Rogachev, X.-H.Jiang, N.N.Fedosenko, E.A.Kulesh*)

Abstract. The paper presents a comparative analysis of the structure and mechanical properties of carbon coatings, highly alloyed with metals Ti, Zr and Al. Coatings were deposited from combined flows of metal and carbon plasma with approximately the same mass content. The influence of the nature of the metal on the size of Csp^2 clusters and the degree of ordering of the carbon matrix has been determined by means of Raman spectroscopy. Using scanning electron microscopy, the features of the morphology of coatings due to the formation of a carbide phase have been evaluated. It is shown that the values of the Young modules (E) and the coefficient of elastic recovery (η) of the coatings are also determined by the nature of the metal phase: a higher hardness is achieved when alloying with titanium, and the η when alloying with aluminum.

Report 30: Polyaniline-based food quality markers (*A.E.Shumskaya, H.A.Novik, T.V.Zhidko, L.V.Filippovich, J.V.Ignatovich, V. Ye. Agabekov, A.A.Rogachev*)

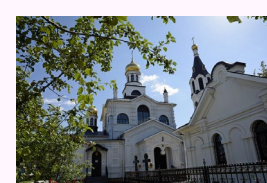
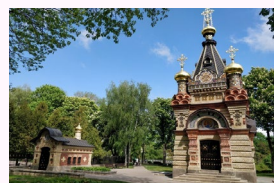
Abstract. Markers have been developed to indicate the quality of food products ((meat, poultry, fish, sausages) on the basis of a nanostructured polyaniline/ copper composite in a polyvinyl alcohol matrix. The marker is a film with a thickness of 15-20 μm . Upon contact with ammonia vapors, they significantly change their optical and electrical characteristics, which are confirmed by UV-, FTIR-ATR spectra and voltammograms. The proposed composite material, as well as PVA films based on it, can be used as an indicator of the presence of ammonia.

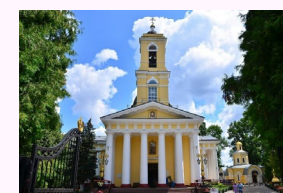
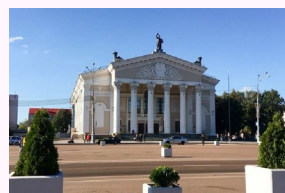
Report 31: Vacuum coatings based on miramistin and their biological properties (*Yiming Liu, I.I.Kontsevaya, A.A.Rogachev, Xiaohong Jiang, M.A.Yarmolenko*)

Abstract. Provides the first studies of genotoxicity and the ability of miramistin-based coatings to stimulate regenerative processes in eukaryotic cells. The coating testing in the Allium cepa system revealed the absence of pathological mitoses beyond the level of normal spontaneous mutation and an increase in the proliferating activity of the meristematic tissue cells in comparison with the control.

Report 32: Synthesis of scintillating glass materials containing yttrium niobate crystallites activated with terbium ions (*M.I.Moskvichyov, V.V.Vaskevich, A.V.Semchenko, V.V.Sidski, V.A.Kravets, V.V.Tkachenko, V.B.Zalessky*)

Abstract. The method for obtaining at reduced temperature sodium boron glass materials containing yttrium niobate crystallites activated with terbium ions was developed. The performed studies of the structural and optical characteristics show the formation of M-YNbO_4 activated by terbium ions with a crystalline phase content of about 95%.





Report 33: Isotropy mechanical properties products with geometry triple periodic minimal surfaces (TPMS) (S.V.Balabanov, A.I.Makogon, K.S.Koshevaya, M.M.Sychev)

Abstract. The impetuous development of science and technology makes ever-higher demands on structural materials. Therefore, the creation of new cellular materials with increased operational characteristics is a relevant task. Cellular structures make it possible to optimize the ratio between material strength and weight. This work presents several research results of the anisotropic mechanical properties of cellular structures with the geometry of triply periodic surfaces (TPMS) produced by additive manufacturing.

Report 34: Behavior of electron-beam irradiated polyethylene and polystyrene (I.Hatescu, C.Borcia, G.Borcia)

Abstract. The influence of electron-beam irradiation on low-density polyethylene (LDPE) and polystyrene (PS) was investigated, aiming to assess the reactions during the irradiation process, as chain scission, chain branching and cross-linking. Under mild irradiation conditions, similar dominant effects, creation of radicals and crosslinking, are shown for the two polymers, although these have different chemical structure and morphology. The crosslinked structure reinforces the rigidity and hardness of the material.

Report 35: Structure and optical properties of a-C coatings doped with nitrogen and silicon (D.G.Piliptsou, A.S.Pobiyaha, A.V.Rogachev, A.S. Rudenkov)

Abstract. Using a pulsed arc discharge, carbon coatings binary-doped with silicon and nitrogen are deposited on quartz and silicon substrates. The structure and phase composition of the coatings are studied by atomic force microscopy, Raman spectroscopy, and X-ray photoelectron spectroscopy. The optic band gap E_g and the refractive index of the coatings are determined depending on the alloying elements. The influence of nitrogen and silicon on the formation of the structure of the carbon matrix and the formation of chemical compounds in the coatings, leading to a change in the width optic band gap E_g , has been established. Changes in the roughness R_a and the size of the Csp^2 cluster are shown in the case of binary doping with nitrogen and silicon.

Report 36: Impact of modeling method on geometry and mechanical properties of samples with TPMS structure (A.I.Makogon, S.V.Balabanov, K.S.Koshevaya, M.M.Sychev)

Abstract. Products based on triply periodic minimal surfaces (TPMS) are promising for use in various applied fields from mechanical engineering to medicine. Despite the fact that TPMS have been known for more than 2 centuries, their practical application became possible only in recent decades with the development of additive technologies. Computer modeling of products based on TPMS for 3D printing is a relevant problem. In this paper impact of modeling method on geometry and mechanical properties of samples with TPMS structure is investigated.

Report 37: Mechanism of double-step conversion reaction in nanostructured tungsten trioxide anode for Li-Ion batteries (R.Bekarevich, Y.Pihosh, Y.Tanaka, K.Nishikawa, Y.Matsushita, T.Hioto)

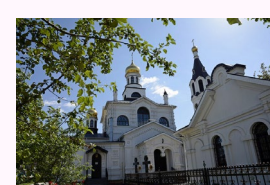
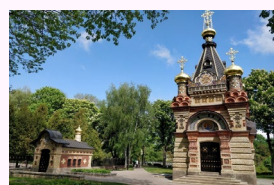
Abstract. Market demands rise the problem of development of lithium-ion batteries (LIBs) with high-energy densities, as LIBs with conventional anodes are limited by low reversible capacity of graphite. Tungsten oxide (WO_3) possessing high theoretical capacity can potentially replace conventional anodes. However, large volumetric changes during the cycling lead to rapid degradation of WO_3 -based electrodes. In this study we report a binder-free nanostructured anode integrated with a current collector. Its controlled geometry minimized volumetric expansion effects and conferred high mechanical stability of anode. Detailed structural analyses supported by theoretical calculations revealed the appearance of the intermediate active phases during conversion reaction.

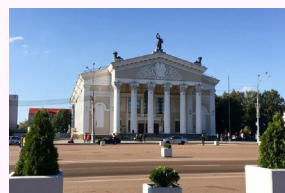
Report 38: Enhancing the seebeck coefficient of Zn-doped MoS_2 grown over carbon fabrics via band engineering (V.Shalini, S.Harish, H.Ikeda, J.Archana, M.Navaneethan)

Abstract. Among various 2D materials, molybdenum disulfide semiconductors have gained much attention in various applications such as electronics, supercapacitors and optoelectronics due to their unique transport properties. But the nature of charge transport remains indefinable as they show lower mobility compared to theoretical values. In the present work, we report a possible method for enhancing the thermoelectric properties of MoS_2 by effectively growing pristine MoS_2 and Zn-doped MoS_2 on carbon fabrics (CFs) by a simple hydrothermal method. The uniform growth of pristine MoS_2 and Zn-doped MoS_2 on CFs was confirmed by structural and morphological analysis. Various concentrations of Zn doped MoS_2 nanosheets grown on CFs showed significant enhancement thermoelectric performances. It was found that the electrical conductivity (1.69×10^2 S/cm) was significantly increased for Sample Zn2 with temperature.

Report 39: Effect of Ag substitution on enhancing the thermoelectric performance of nanostructured SnSe (K.Kalaianarasan, D.Sidharth, A.S.Alagar Nedunchezian, P.Rajasekaran, M.Shimomura, M.Arivanandhan, H.Ikeda, Y.Hayakawa, R.Jayavel)

Abstract. Nanostructured $Sn_{1-x}Ag_xSe$ ($x=0.02, 0.04, 0.08$) materials were synthesised via mechanical milling followed by hydrogen decrepitation method. The structural, morphological, compositional and thermoelectric properties were investigated. The XRD analysis confirmed the crystal structure of SnSe. The prepared $Sn_{1-x}Ag_xSe$ samples were pelletized via high pressure high temperature sintering (HPHTS) technique for thermoelectric measurements. Seebeck coefficient and electrical resistivity were measured as a function of temperature. It was found that the power factor of $Sn_{0.92}Ag_{0.08}Se$ was 6.3 times higher than that of pristine SnSe.





Report 40: Investigation on influence of Cu doping on thermoelectric performance of tin-selenide-based nanostructures (S.Athithya, H.Ikeda, M.Navaneethan, S.Harish, J.Archana)

Abstract. Tin selenide (SnSe) has attracted more interest as thermoelectric material due to the anharmonic nature and anisotropy. Thus, a high ZT of 2.6 has been achieved for single crystalline SnSe. We have explored the effect of Cu doping on the nanostructured SnSe synthesized via ball milling method. The presence of Cu as well as nanostructuring plays a crucial role in reducing thermal conductivity and enhancing power factor compared with pristine SnSe. Cu⁺ ions provide more hole carriers, which leads to enhance the electrical conductivity. The higher doping concentration of Cu contributes to a lower thermal conductivity of around 0.85 W/mK at 280 K, which is improved by one order of magnitude compared with pristine SnSe 1.8 W/mK at 280 K.

Report 41: Characteristics of nanocomposite sol-gel films on black silicon surface (A.V.Semchenko, V.V.Sidski, O.I.Tyulenкова, V.E.Gaishun, D.L.Kovalenko, G.Y.Ayvazyan, L.A.Hakhoyan)

Abstract. The structural and photoelectric characteristics of thin sol-gel ZnO, TiO₂, and SiO₂ films on the black silicon (b-Si) surface have been studied. It has been shown that it is preferable to use ZnO and TiO₂ films as passivating and protective films of solar cells based on b-Si, which have stable structural and optical properties and, at least, do not worsen the reflection of b-Si in the near infrared and visible regions of the solar radiation.

Report 42: AFM topography of ZnO_x:MgO nanocomposite sol-gel films on the surface of silicon (V.V.Sidski, V.V.Malyutina-Bronskaya, S.A.Soroka, A.V.Semchenko, K.D.Danilchenko, O.I.Tyulenкова, V.A.Pilipenko)

Abstract. The results of determining by AFM the parameters of sol-gel synthesis influence for the formation of nanocomposite coatings ZnO_x:MgO with a band gap greater than 5 eV and with high sensitivity to UV and visible radiation are presented. It is shown that depending on the magnesium concentration change in the surface of the ZnO_x: Mg films is observed.

Report 43: Sol-gel synthesis TiO₂ nanotubes based on ZnO nanorods, for use in solar cells (D.L.Kovalenko, M.Dobromir, V.V.Vaskevich, A.V.Semchenko, D.Luca, V.V.Sidski, O.I.Tyulenкова, Ya.A.Kosenok)

Abstract. In the paper, the sol-gel method for obtaining TiO₂ nanotubes on a sublayer of ZnO nanorods is described. The ZnO nanorod layer was pre-formed by the hydrothermal method. Optimal regimes have been determined for the formation TiO₂-ZnO structures. An extended surface nano-morphology study of the obtained materials has been carried out.

Report 44: NiO and NiO:Al films for solar cells: a compromise between electrical conductivity and transparency (V.V.Filippov, I. A.Kashko, A.K.Tuchkovskii, D.L.Kovalenko, V.V.Vaskevich, V.E.Gaishun)

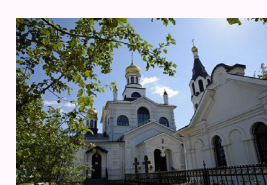
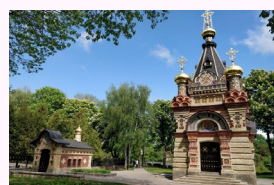
Abstract. The paper presents sol-gel and thermal oxidation methods for producing thin NiO films. The high transparency of the films correlates with their low electrical conductivity. Small additions of Al can significantly increase the conductivity of the films, while the transparency of the films is determined by the oxidation/annealing temperatures.

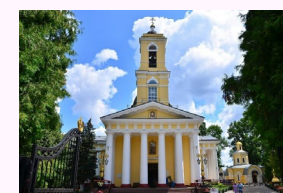
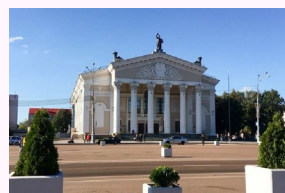
Report 45: The effect of SiO₂ content rate in simulated lunar regolith on ablation plume temperature and the feasibility assessment of Al₂O₃ reduction (Kazune Uesugi, Kanta Ishiguro, Ryohei Oishi, Makoto Matsui)

Abstract. We considered the application of lunar regolith for the construction of a lunar base. To obtain aluminum as building materials, the reduction of simulated lunar regolith composed of alumina and silicon dioxide was performed using 1-kW-class continuous-wave diode laser ablation. The temperature dependence of the ablation plume on the content rate of silicon dioxide was investigated, and irradiated surface analysis was conducted using EDX. In addition, the same experiment was conducted with a mixture of silicon and alumina. The silicon dioxide and silicon ratio were set to 25-50%, respectively. The plume temperature and Al(I) spectra decreased with silicon dioxide ratio, but not for silicon. EDX results did not show any reduction of alumina in the simulated regolith but did detect aluminum in the silicon mixture.

Report 46: Development of sapphire-like glass by sol-gel technology (D.L.Kovalenko, V.E.Gaishun, V.V.Vaskevich, N.A.Aleshkevich, Ya.A.Kosenok, O.I.Tyulenкова, O.V.Ignatenko)

Abstract. This paper describes the selection of research conducted precursors and methods for converting them to the optically transparent aluminum oxide, identified the most promising options for synthesis sapphire-like glasses.





Section “Measurement, identification, and control”

Report 47: Discovering the Sicilian byzantine icons through a combination of imaging and spectroscopic techniques (*Francesco Armetta, Veronica Ciaramitaro, Gabriella Chirco, Giuseppe Lo Re, Massino Midiri, Dariusz Hreniak, Eugenio Caponetti, Maria Luisa Saladino*)

Abstract. The iconographic heritage is one of the treasures of Byzantine art and spirituality that enrich Sicily (Italy) since the early 16th century. In this work, for the first time, an investigation of some Sicilian Icons of Greek-Byzantine origin is reported. The diagnostic studies were carried out by using non-invasive Imaging techniques such as photography (grazing vis-light, UV Fluorescence, Infrared, Infrared False Color), Radiography, and Computed Tomography and Spectroscopic techniques such as X-ray Fluorescence, Infrared and UV-vis Reflectance Spectroscopy. The identification of the constituents (support, pigments and binders) provides a decisive contribution to the correct historical and artistic placement of the Icons, treasure of east Europe historical community in Sicily. Furthermore, the obtained information allows to define their conservation state, the presence of foreign materials and to drive their protection and restoration for future prospective.

Section “Metamaterials and metasurfaces”

Report 48: Modeling a three-spike absorber in the range 9-13 GHz (*D. Slepiankou, A.Balmakou, S.Khakhomov, I. Semchenko*)

Abstract. The aim of this work is to model and theoretically describe an absorbing metamaterial consisting of an array with holes and discs. The simulation is implemented in the Ansys HFSS software product. This work is a preliminary result. Based on this work, we will try to simulate and then create a metamaterial in the 1-6 GHz range.

Report 49: Production and experimental study of a weakly reflecting absorbing metamaterial based on planar spirals in the microwave range (*I.Semchenko, A.Samofalov, A.Kravchenko, S.Khakhomov*)

Abstract. The work aims to produce and experimentally study an absorbing and at the same time weakly reflecting metamaterial consisting of conducting planar two-turn spirals on a dielectric substrate. Such a pre-designed metamaterial is manufactured within the framework of printed circuit board technologies.

Report 50: Optical chirality enhancement with dielectric metasurfaces (*I.A.Faniayeu, I.A.Fanyaev and V.S.Asadchy*)

Abstract. In this work, we numerically investigate the generation of superchiral fields with achiral dielectric metasurface for further enhancement of CD signals from chiral molecules. The high-refractive-index dielectric metasurface is used to enhance localized electric and magnetic fields simultaneously inside the disk under the CPL excitation at visible wavelengths. As a result, the spatially overlapped electric and magnetic fields with an appropriate phase condition lead to the generation of superchiral fields that in a result maximized optical chirality. The design of a dielectric metasurface consists of TiO₂ disks arranged into a lattice with a period of 450 nm. By changing the diameter of the disk with remaining the height ($h = 195$ nm), we can spatially overlap electric and magnetic fields. Due to the low lossy TiO₂ invisible range, the transmittance of metasurface with optimized parameters ($d = 200$ nm) at the wavelength of 598 nm tends to one while the reflection remains zero. Meanwhile, the optical chirality enhancement reaches up to 485-fold, which can amplify the CD signal from molecules by over two orders of magnitude. We believe that our work could inspire novel on-chip photonic components for surface-sensing in CD spectroscopy, enantioselectivity, and sorting applications.

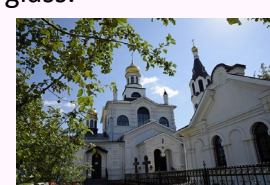
Section “Modeling and diagnostics”

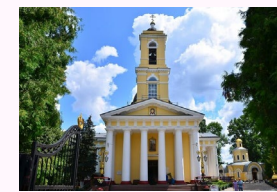
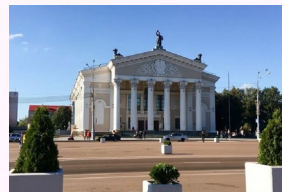
Report 51: Simulation of laser splitting of bilayer structures made of silicon wafers and glass substrates (*Y.V.Nikitjuk, A.N.Serdyukov, I.Y.Aushev*)

Abstract. The paper presents the results of a finite-element simulation of the laser splitting process of bilayer structures of monocrystalline silicon and glass under the influence of laser beams with wavelengths equal to 0.808 μ m and 10.6 μ m and a refrigerant on the workpiece. The calculation of thermoelastic fields formed in a bilayer wafer as a result of laser heating was performed for three cuts of silicon crystals, i.e. (100), (110), (111). The outcomes of this research can be used to optimize the process of laser separation of bilayer structures of monocrystalline silicon and glass.

Report 52: The use of artificial neural networks for determining the parameters of laser processing of fused quartz (*Y.V.Nikitjuk, A.N.Serdyukov, V.A.Prokhorenko, I.Y.Aushev*)

Abstract. This paper provides the simulation of the laser splitting process of fused quartz using artificial neural networks. The calculations of temperatures and thermoelastic stresses were performed by the finite element method in the ANSYS program to create a training data array and an array data for testing neural networks. The paper studies the influence of neural network architecture, the size of the training data array, and the training time on the accuracy of determining thermoelastic stresses and temperatures in the zone of laser processing of quartz sol-gel glass.





Report 53: Optimization of quartz glass laser polishing parameters using the computational experiment planning method (V.A.Emelyanov, E.B.Shershnev, Y.V.Nikitjuk, S.I.Sokolov)

Abstract. This paper demonstrates the optimization of the laser polishing process of quartz glass. It was performed using the method of a complete factorial experiment with a two-level variation of factors and the parameters search method. After simulation, the laser polishing modes of quartz glass have been determined. These modes ensure the temperature set points in the processing zone at the minimum values of thermoelastic stresses in quartz plates.

Report 54: Characterization of laser welding of steel 30XГCH2A by combining artificial neural networks and finite element method (Y.V.Nikitjuk, G.A.Bayevich, V.N.Myshkovets, A.V.Maximenko, I.Y.Aushev)

Abstract. The paper presents the calculation of the temperature fields, created at different depths, via artificial neural networks and the finite element method during laser welding of steel 30XГCH2A. The training data array and the array data for testing neural networks were created using ANSYS.

Report 55: Investigation of acoustic wave propagation in complex geometry (M.Yu.Arsentev, E.I.Sysoev, A.I.Makogon)

Abstract. The study of the interaction of acoustic waves with objects of complex geometry is a topic of significant interest in many areas of science and engineering, including aeroacoustics, civil industries, and in military and defense applications, particularly for detection and survivability. In this work, using stable and explicit second order accurate finite difference method for the elastic wave equation, we investigated the propagation of acoustic waves in such samples (material - corundum). The results of the study show how the wave being reflected from the walls and refracted. Ultimately, active absorption of the wave amplitude and sound pressure was observed.

Report 56: Development of material for 3D printing based on thermoplastic elastomer (M.V.Timoshenko, S.V.Balabanov, M.M.Sychev, D.I.Nikiforov)

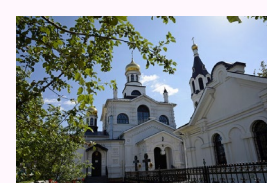
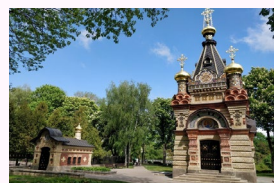
Abstract. Thermoplastic elastomer based on styrene-butadiene rubber was developed for 3D printing using fused deposition modelling. 3D modeling of simple and complex geometric structures from the developed material is performed. Optimal 3D printing parameters for this material were obtained.

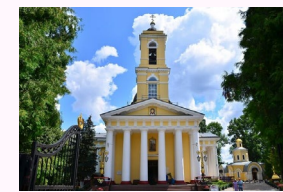
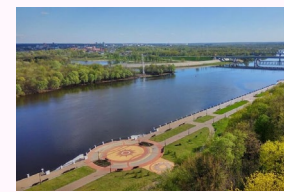
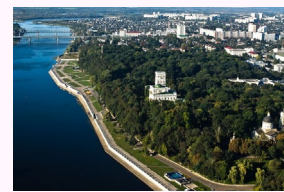
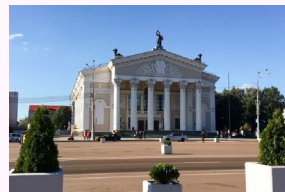
Report 57: Investigation of the effect of observation window on the sensitivity enhancement in the multi-pass cell outside the expansion wave tube chamber (Ryuji Kobayashi, Hiroaki Sakai, Makoto Matsui)

Abstract. Although expansion tubes have been used to simulate atmospheric entry environment, the flow conditions have not been completely characterized. In our previous research, the sensitivity of laser absorption spectroscopy (LAS) using multi-pass cell outside the chamber was not high enough to diagnose ISAS/JAXA expansion tube flows because the inclination of the observation window. In this study, the sensitivity enhancement of multi-pass cells in the inclination of interior cell window was investigated by calculation using the ray-tracing method considering laser spread. As a result, the higher the sensitivity, the smaller the acceptable range of slope. The inclination tolerance of the observation window is larger than the inclination tolerance of the concave mirror.

Report 58: Modeling and optimization of a microgrid for a midrise apartment and industry (Rituraj Rituraj and Annamaria R. Varkonyi-Koczy)

Abstract. To meet the energy demand of an area having a midrise apartment and industry, a microgrid model is proposed and its sensitivity analysis is performed to access the impact of fuel price on the least-cost system design. The proposed microgrid system is having an overall energy consumption of 24,188 kWh/day and 2129 kW during a peak time. The original grid search algorithm and proprietary derivative-free algorithm are used to simulate all of the feasible system configurations defined by the search space and to search for the least-costly system respectively. On this basis, estimation for the lifecycle cost of the system, accounting for the capital, replacement, operation and maintenance, fuel, and interest costs are discussed. The result shows an efficient rate of return on investment and the internal rate of return for the designed microgrid is 72.6% and 75.9% respectively. The simulation result of the HOMER optimization tool showed that a PV-diesel system with battery storage will be most cost-effectively supply the energy required by the given setup. The achieved result shows hourly energy flows for each component as well as annual cost and performance summaries.





Section “Multimedia and E-learning techniques and materials”

Report 59: Online lesson “Academic English I” for students (*Satoshi R. Ota*)

Abstract. Since 2019, I have been providing technical support for the required third year students’ class "Academic English I" in the Department of Electrical and Electronic Engineering, Faculty of Engineering, Shizuoka University. The teaching team includes Professor Damon M. Chandler (Now Ritsumeikan University) of the Department of Electrical and Electronic Engineering and Professor Emerita Valerie A. Wilkinson of the Faculty of Informatics, Shizuoka University. It was a face-to-face lecture in 2019, but an online lecture was held in 2020 and 2021 due to the spread of the new coronavirus infection (COVID-19). I report on the results of questionnaires to students and faculty members from the preparation for the online lecture to the implementation as well as post-lecture feed-back, and after the lecture. We used Moodle system "LecShizu" to checked student’s attendance and so on.

Report 60: Project architecture and data model for AR application development (*Aksionova Natallia*)

Abstract. Augmented reality is an intuitive approach in displaying models. Instead of controlling position and rotation of virtual camera with primitive controls, users are enabled to look at the model by inspecting them through cameras of their devices. Since this project represents an SDK, project structure appears as a set of files and instructions how to use them. In order to implement architecture that is easy to use and maintain, separation of concerns principle should be used during architecture planning. This will enable users of this library to only use functionality they need, which also corresponds to Single-responsibility principle.

Section “Nanotechnology and nanometrology”

Report 61: Localized surface plasmon resonance liquid sensors based on array gold nanoparticles fabricated on 36XY-LiTaO₃ substrate (*Teguh Firmansyah, Gunawan Wibisono, Eko Tjipto Rahardjo and Jun Kondoh*)

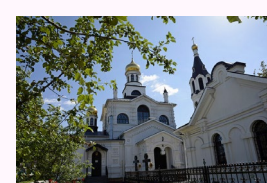
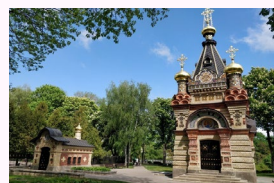
Abstract. Localized surface plasmon resonance (LSPR) has excellent performance for sensor application. It usually composes base on metal nanoparticle (MeNP) and deposited it on a glass substrate. Therefore, the primary application has focused on refractive index sensors only. As a novelty, we propose to develop an LPSR sensor based on an array of gold nanoparticles (AuNPs) fabricated on 36XY-LiTaO₃, which is a piezoelectric substrate. Complete data such as plasmonic electric field (E-field) simulation, fabrication devices, and implementation as sensor data were provided. Finally, the proposed method has functions for bridging between LSPR and piezoelectric material.

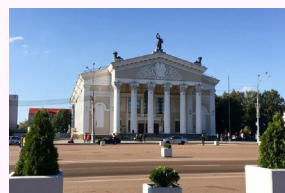
Report 62: Atomic force spectroscopy experiments with amino-functionalized silicon AFM tips and samples (*L.Sirghi, A.Besleaga*)

Abstract. Nanoscopic probes in scanning probe microscopy interact with the target surfaces through forces that are vital to applications in microscopy imaging and single-molecule studies of biologic forces. At their turn, the interaction forces depend crucially on the chemistry of probe and sample surfaces. Therefore, controlling and modification of the surface chemistry of the nanoscopic probes is vital for the success of these microscopic studies. The present work uses plasma technology in combination with wet-chemistry functionalization methods to functionalize silicon atomic force microscopy (AFM) probe and sample surfaces with amino (-NH₂) chemical groups. Plasma cleaning, oxidation, and hydroxylation processes are used to chemically activate silicon or silicon nitride surfaces by generating surface silanol (Si-OH) groups. This process is followed by self-assembled monolayer (SAM) deposition of ethanolamine to generate surface amino groups. The amino-functionalized AFM probes and samples were used in atomic force spectroscopy measurements that confirmed successful functionalization by chemical force titration.

Report 63: Heat treatment effect on the mechanical properties of nanostructured carbon coatings (*A.S.Rudnikov, A.S.Pobiyaha*)

Abstract. The effect of heat treatment temperature on the microhardness and tribotechnical properties of carbon coatings, formed from the plasma of a pulsed cathode-arc discharge on a polyacrylamide sublayer, has been determined. The heat treatment of carbon-based systems leads to a decrease in their microhardness and friction coefficient with a simultaneous increase in the volumetric wear coefficient of the counterbody. It is due to sp³→sp² phase transitions and CN_x-type compounds arising through cyclization processes during heat treatment.





Report 64: Raman investigation of multiferroic BiFeO_3 and $\text{Bi}_{1-x}\text{Sm}_x\text{FeO}_3$ materials synthesized by the sol-gel method (*O.Fesenko, T.Tsebriienko, A.Yaremkevych, V.V.Sidski, A.V.Semchenko, V.E.Gaishun, D.L.Kovalenko, S.A.Khakhomov*)

Abstract. The present work presents the results of the investigation of multiferroic materials (BiFeO_3 and $\text{Bi}_{1-x}\text{Sm}_x\text{FeO}_3$) with perovskite structure, which possesses two types of orderings: ferromagnetic and ferroelectric. Also, the obtained samples were investigated by Raman spectroscopy to provide detailed information about chemical structure, phase purity and polymorphism, crystallinity and molecular interactions. To enhance the magnetoelectric interaction of bismuth ferrite samples, Bi cations were substituted by isovalent Sm cations with the formation of systems with the general formula $\text{Bi}_{1-x}\text{Sm}_x\text{FeO}_3$, where $x = 7.0; 10.0; 20.0$ and 25.0 . The interest was to study the features of the formation of ferromagnetic composites both in the form of powders and in the form of films on a silicon substrate, as well as to explore the effect of the formation method on their magnetoelectric properties.

Report 65: Piezoelectric properties of $\text{SrBi}_2(\text{Ta}_x\text{Nb}_{1-x})_2\text{O}_9$ thin films synthesized by the sol-gel method (*A.V.Semchenko, V.V.Sidski, O.I.Tyulenkov, A.Yu.Shepelina, D.A.Kiselev, V.A.Pilipenko*)

Abstract. The present work aims to design and study novel functional thin films with ferro- and properties. $\text{SrBi}_2\text{Ta}_2\text{O}_9$ and $\text{SrBi}_2(\text{Ta}_x\text{Nb}_{1-x})_2\text{O}_9$ thin films were synthesized by sol-gel method on Pt/Ti/SiO₂/Si substrates. The influence of the synthesis conditions and the presence of niobium on the features of the piezoelectric properties were determined. The PFM method was applied to visualize not only the morphology of grains, but also their local piezoelectric activity.

Report 66: Photocatalytic activity and wettability of TiO_2 nanotube arrays coupled with WO_3 and ZnO (*C.T. Konrad-Soare, M.Dobromir, G.Stoian, M.Luca, A.Ciobanu, D.Luca*)

Abstract. New results are presented in this work on the photocatalytic performance of modified titanium dioxide (TiO_2) nanotube arrays, prepared via electrochemical anodization. TiO_2 semiconductors have a band gap value (3.2 eV), which make them suitable as photoactivated catalysts. For surface activation, UV-A radiation (315 – 400 nm) can be used. By depositing WO_3 and ZnO nano-coatings on top of titania surface, formation of oxide semiconductor heterojunctions has been reported, with the benefit of longer electron-hole pairs lifetime, due to reduced recombination rate inside such structures. Here, we focus our investigation on titania nanotube arrays (TNA) loaded with zinc and tungsten oxide ultra-thin layers. On macroscale, loading TNA with WO_3 and ZnO layers led to significantly time-prolonged photocatalytic activation and, thus, the catalytic performance.

Report 67: Two-steps formation of ZnO -loaded TiO_2 nanotube array films with enhanced photocatalytic performance (*M.Dobromir, C.T.Konrad-Soare, R.P.Apetrei, A.Airinei, A.V.Semchenko, D.L.Kovalenko, D.Luca*)

Abstract. Recent results are reported on the investigation of the optical properties of ZnO -loaded TiO_2 nanotubes array layers. TiO_2 nanotubes layers formed by electrochemical anodization of the Ti surface were subsequently loaded with controllable amounts ZnO , originating from a magnetron sputtering source. Structural and optical analyses of the ZnO - TiO_2 composite films with different ZnO coverage were carried out to further investigate the electronic properties of the composite films. The results are discussed in terms of the occurrence of the ZnO - TiO_2 heterojunctions and the modification of band gap. These effects increase the photocatalytic yield and activation duration of the films.

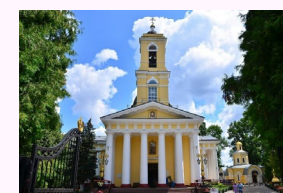
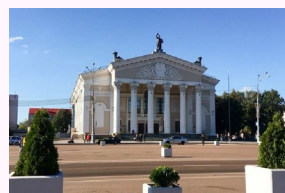
Report 68: Atomic force microscopy indentation of supported lipid bilayers (*G.Tifui, S.Teodoroff-Onesim, L.Sirghi*)

Abstract. Because of the small size of the cells, investigation at the sub-cellular level of their physical properties remains difficult. Atomic force microscopy (AFM) has proved to be a valuable technique used not only to acquire high-resolution 3D topography of cell surface, but also to measure locally the elastic and hardness properties of cells by using the AFM instrument as a nanoindentation tool. In this work, AFM indentation experiments of supported lipid bilayers (SLB) on mica are performed to investigate their hardness. In such measurements, the strain response of the SLB to the compression stress applied by the sharp tip of the AFM probe (curvature radius of 10 nm) is analyzed. It was observed that under the compression stress, the SLB deformed first elastically and then plastically (with a lateral disruption of the lipid bilayer). Transition between elastic and plastic deformation is characterized by the SLB breakthrough force. It is shown that plasma hydroxylation of the AFM tips decreases slightly the SLB breakthrough force.

Report 69: Studies of magnesium – hydroxyapatite micro/nano film for drug sustained release (*Jinxing Cao, Xiaohong Jiang, A.V.Rogachev*)

Abstract. It is challenging to fabricate the bioactive films containing magnesium (Mg) particles to obtain a film with porous structure. These microporous structures facilitate the diffusion of the drug covered by the Mg-HA film to achieve sustainable drug release. Herein, ciprofloxacin hydrochloride (CIP) film as the drug representative is obtained by low energy electron beam deposition (LEBD) to verify the sustained release effect of Mg-HA film. Therefore, the four-layer composite films with a distribution of the CIP are obtained using the layered growth of CIP film and Mg-HA film by the PLD-LEBD coupling technology. The results showed that Mg-HA film not only prolonged the CIP release period, but also enhanced the drug release in the middle and late stage.





Section “Photonics”

Report 70: High power terahertz wave emission using DAST crystal (*T.Kawauchi, G.Ohtake, C.Koyama, H.Uchida, K.Takeya and S.R.Tripathi*)

Abstract. The power of terahertz wave emitted by non-linear optical crystal via optical rectification of femto-second laser pulses depends upon the power of the laser used to pump the optical crystal. However, significant amount of pump power is lost due to Fresnel’s reflection at air-crystal boundary during this process. In this study, we used the anti-reflection (AR) coat known as cytop on the surface of non-linear crystal 4-Dimethylamino-N-methyl-stilbazolium tosylate (DAST), which enabled to increase the incident pump power. The power of terahertz wave generated by DAST crystal with AR coating is higher than the power of terahertz wave generated by the crystal without AR coating.

Section “Plasma physics”

Report 71: The physicochemical/electrical properties of plasma activated medium by dielectric barrier discharge microplasma (*A.G.Yahaya, T.Okuyama, J.Kristof, M.G.Blajan and K.Shimizu*)

Abstract. Plasma activated medium (PAM) is a relatively new approach for bacterial inactivation while ensuring safety and maintaining the properties of the material to be sterilized. Recent research reported that PAM is effective for bacterial sterilization up to 8 log reductions in CFU/mL. In this paper, further physicochemical/electrical properties of PAM generation by dielectric barrier discharge microplasma (DBD) were investigated at relatively low discharge voltage. Temperature, water lost, pH, UV-VIS absorbance after 2 months, nitrite/nitrate concentration, resistivity and conductivity were assessed after treatment. The results suggested that microplasma treatment of PAM causes increase in resistivity, acidification, dissolved reactive oxygen and nitrogen species (RONS), creating an environment suitable for sterilization of bacteria. These properties could be preserved for long time under low temperature. Therefore, PAM is an effective method for surface sterilization.

Report 72: Velocity distribution functions at plasma boundary (*C.Costin*)

Abstract. The study of bounded laboratory plasmas often requires the knowledge of particle distribution function at the plasma boundary. The distribution function can describe either plasma particles that are reflected on the surrounding surfaces or particles that are injected in plasma due to different surface phenomena: thermionic emission, secondary emission, sputtering etc. The distribution function is usually defined as a combination of two independent distributions, one angular and one energy dependent. In the current study, all distributions are discussed as functions of the velocity components. Different combinations of angular (isotropic and cosine-type) and energy (energy dependent, uniform, and mono-kinetic) distributions are compared based on their effect on subsequent calculations.

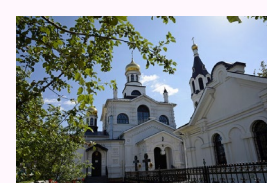
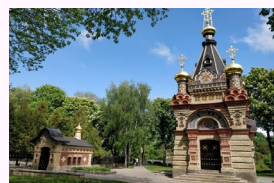
Report 73: Oxidation and stability of polymers treated by atmospheric-pressure plasma (*E.Bîrleanu, I.Mihaila, I.Topala, G.Borcia*)

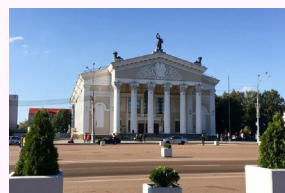
Abstract. The influence of atmospheric-plasma exposure on various polymers is studied, aiming to evaluate the plasma capability for efficient, uniform and stable surface modification. The surfaces show strong increase of the hydrophile character, related to incorporation of oxygen groups. The limiting level of modification is similar for all polymers, whereas the post-treatment stability is better for non-polar polymers, as PE and PS.

Sections “iA Young Researcher”

Report 74: Diamond radiation detector with built-in boron-doped neutron converter layer (*T.Miyake, H.Nakagawa, T.MASUZAWA, T.Yamada, T.Nakano, K.Takagi, T.Aoki and H.Mimura*)

Abstract. We report on the fabrication and characterization of a solid-state neutron detector made of polycrystalline diamond, grown by hot-filament chemical vapor deposition (HFCVD). The detector consists of undoped free-standing polycrystalline diamond layer and a heavily boron (B)-doped polycrystalline diamond top layer that serves as an electrical contact and a converter for neutron-alpha conversion, respectively. The boron impurity captures (thermal) neutrons and generates alpha particles, which excite electron-hole pairs in the diamond detector to form signal pulse current. Detection of radiation particles was demonstrated using alpha particles from americium-241.





Report 75: Spatial resolution of X-ray imaging using 80 μ m pitch TlBr detector (Kohei Toyoda, Katsuyuki Takagi, Hiroki Kase, Toshiyuki Takagi, Kento Tabata, Tsuyoshi Terao, Hisashi Morii, AKifumi Koike, Toru Aoki, Mitsuhiro Nogami, Keitaro Hitomi)

Abstract. This study introduces an X-ray imager that uses TlBr detectors and demonstrates its potential for X-ray imaging applications. Although TlBr detectors are suitable for X-ray imaging applications because of the associated large attenuation coefficients and direct conversion behavior, realizing a flat-panel detector with TlBr involves developing processes. The proposed imager is constructed utilizing a combination of existing technologies; it comprises a plate electrode containing thallium metal to suppress the polarization phenomenon, pixelated silver electrodes with 80 μ m pitch, and a photon-counting-type readout integrated circuit (ROIC) that can work in the hole as well as electron collection modes. The modulation transfer function (MTF) of the imager is calculated based on the imaging results of an X-ray test chart, and the result corresponds to 180 μ m sampling. The measured high-MTF shows the immense potential of TlBr detectors for X-ray imaging applications.

Report 76: Numerical solution of the two-dimensional Logunov-Tavkhelidze equation with the sum of two separable potentials in the momentum representation (A.V.Paulenko, Yu.A.Grishechkin)

Abstract. A numerical solution of the two-dimensional quasipotential Logunov-Tavkhelidze equation describing the bound states of systems of two identical scalar particles when simulating their interaction by the sum of two separable potentials in the momentum representation is found. The results obtained are illustrated by plots of the dependences of the partial wave functions and the energy of the system on the momentum and the coupling constant, respectively. It was found that there is only one bound state, and the partial wave functions have an infinite number of zeros when separable potentials are taken into account.

Report 77: Partial two-particle equations in the relativistic configurational representation for scattering p-states in the case of a superposition of two δ -function potentials (V.N.Kapshai, A.A.Grishechkina)

Abstract. Exact solutions of two-particle equations are considered in the relativistic configurational representation for scattering p-states in the case of superposition of two δ -function potentials. Scattering amplitudes and cross sections are determined. Comparative analysis is carried out with the case of scattering s-states.

Report 78: Green functions of relativistic quasipotential equations for complex values of energy (A.V.Buzhan, V.N.Kapshai)

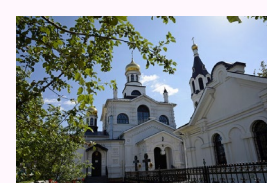
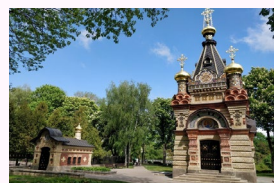
Abstract. Green functions of quasipotential equations for scattering states of a two-particle system are investigated for complex values of energy. Green functions of quasipotential equations in the relativistic configurational representation for complex values of energy are found. Limits for implementing complex-scaling method or investigating resonance states of scattering cross sections of a relativistic two-particle system are defined.

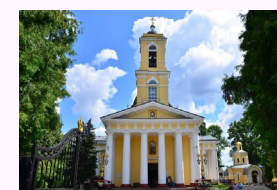
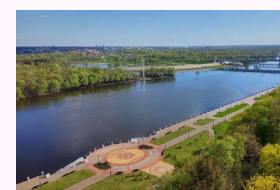
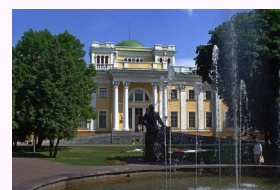
Report 79: Analysis of the spatial distribution of the second-harmonic radiation generated in a thin surface layer of a spheroidal dielectric particle (V.N.Kapshai, A.A.Shamyna, A.I.Tolkachev)

Abstract. Based on Rayleigh-Gans-Debye model, the spatial distribution of the second-harmonic radiation generated in a thin surface layer of a spheroidal dielectric particle is presented using three-dimensional directivity patterns. The peculiarities of the forms of the directivity patterns are described for the key values of the parameters. The symmetries of the directivity patterns are revealed, as in the case of second-harmonic generation in a surface layer of a spherical particle. The dependence of the polarization of the generated radiation on the polarization of the incident wave is described.

Report 80: Maxima of the power density of the second-harmonic generation from a linear structure of long cylindrical dielectric particles (V.N.Kapshai, A.I.Talkachov, A.A.Shamyna)

Abstract. The problem of second-harmonic generation by a plane electromagnetic wave from a linear structure of long cylindrical dielectric particles coated by an optically nonlinear substance is solved in the far field in the Rayleigh-Gans-Debye approximation. The directions in which there occurs maximal intensity of the generated radiation and the directions in which there occurs no generation are found. It is revealed that the maximal power density of second harmonic generation from the structure is proportional to the square of the number of cylinders.





Author index

Aarthy M.

[Report 16:](#) High-performance and low-voltage current sense-amplifier using GAA-CNTFET with different chirality and channel
(THURSDAY 21 October, Hall 5, 13.30-15.00, poster section)

Abdilalizadeh L.

[Report 1:](#) Investigating urban sustainability by emphasizing on the approaches for reducing fuel consumption using intelligent transportation system
(WEDNESDAY 20 October, Hall 2, 11.00-13.00)
[Report 2:](#) Environmental risk management by achieving sustainable development goals in architecture and urban engineering
(WEDNESDAY 20 October, Hall 2, 11.00-13.00)

Agabekov V.Ye.

[Report 4:](#) Application of additive technology to create universal carriers of cellular structures (WEDNESDAY 20 October, Hall 4, 13.30-15.00, poster section)
[Report 30:](#) Polyaniline-based food quality markers (WEDNESDAY 20 October, Hall 1, 11.00-13.00)

Airinei A.

[Report 67:](#) Two-steps formation of ZnO-loaded TiO₂ nanotube array films with enhanced photocatalytic performance
(WEDNESDAY 20 October, Hall 3, 11.00-13.00)

Aksionova N.

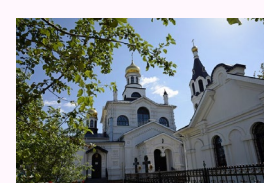
[Report 60:](#) Project architecture and data model for AR application development (THURSDAY 21 October, Hall 3, 10.00-13.00)

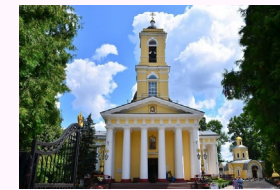
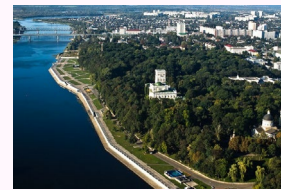
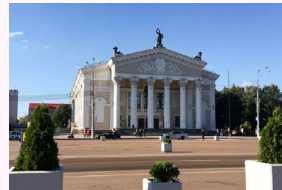
Alagar Nedunchezian A. S.

[Report 39:](#) Effect of Ag substitution on enhancing the thermoelectric performance of nanostructured SnSe (THURSDAY 21 October, Hall 1, 10.00-13.00)

Aleshkevich N. A.

[Report 46:](#) Development of sapphire-like glass by sol-gel technology (THURSDAY 21 October, Hall 1, 10.00-13.00)





Andrieieva O. L.

Report 26: Investigation of the convection effect on the inclusion motion in thermally stressed crystals
(WEDNESDAY 20 October, Hall 8, 13.30-15.00, poster section)

Aoki T.

Report 8: Analysis of color coordinates in dried blood spots under aging for forensic medical applications (WEDNESDAY 20 October, Hall 2, 11.00-13.00)
Report 12: Evaluation of radiation detection characteristics by α -Ga₂O₃ (THURSDAY 21 October, Hall 2, 10.00-13.00)
Report 21: Applications for effective representation of imaging with X-ray CT (THURSDAY 21 October, Hall 9, 13.30-15.00, poster section)
Report 24: Research of morphology and luminescence of particles based on yttrium fluorides for medical usage
(WEDNESDAY 20 October, Hall 7, 13.30-15.00, poster section)
Report 26: Investigation of the convection effect on the inclusion motion in thermally stressed crystals
(WEDNESDAY 20 October, Hall 8, 13.30-15.00, poster section)
Report 74: Diamond radiation detector with built-in boron-doped neutron converter layer (FRIDAY 22 October, Hall 1, 10.00-12.00)
Report 75: Spatial resolution of X-ray imaging using 80 μ m pitch TlBr detector (FRIDAY 22 October, Hall 1, 10.00-12.00)

Apetrei R. P.

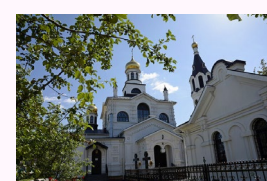
Report 67: Two-steps formation of ZnO-loaded TiO₂ nanotube array films with enhanced photocatalytic performance
(WEDNESDAY 20 October, Hall 3, 11.00-13.00)

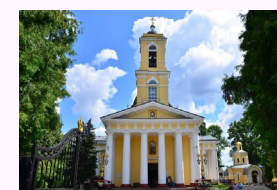
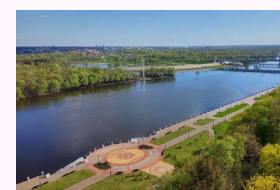
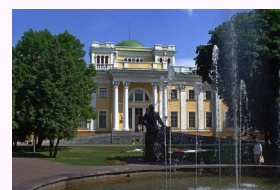
Archana J.

Report 38: Enhancing the seebeck coefficient of Zn-doped MoS₂ grown over carbon fabrics via band engineering
(WEDNESDAY 20 October, Hall 11, 13.30-15.00, poster section)
Report 40: Investigation on influence of Cu doping on thermoelectric performance of tin-selenide-based nanostructures
(THURSDAY 21 October, Hall 10, 13.30-15.00, poster section)

Ardabili S.

Report 1: Investigating urban sustainability by emphasizing on the approaches for reducing fuel consumption using intelligent transportation system
(WEDNESDAY 20 October, Hall 2, 11.00-13.00)
Report 2: Environmental risk management by achieving sustainable development goals in architecture and urban engineering
(WEDNESDAY 20 October, Hall 2, 11.00-13.00)





Armetta F.

[Report 47:](#) Discovering the Sicilian byzantine icons through a combination of imaging and spectroscopic techniques
(THURSDAY 21 October, Hall 2, 10.00-13.00)

Arivanandhan M.

[Report 39:](#) Effect of Ag substitution on enhancing the thermoelectric performance of nanostructured SnSe (THURSDAY 21 October, Hall 1, 10.00-13.00)

Arsentev M. Yu.

[Report 55:](#) Investigation of acoustic wave propagation in complex geometry (THURSDAY 21 October, Hall 3, 10.00-13.00)

Asadchy V. S.

[Report 50:](#) Optical chirality enhancement with dielectric metasurfaces (THURSDAY 21 October, Hall 15, 13.30-15.00, poster section)

Athithya S.

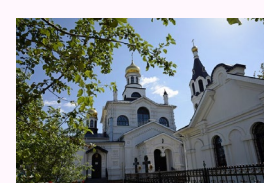
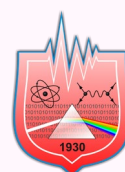
[Report 40:](#) Investigation on influence of Cu doping on thermoelectric performance of tin-selenide-based nanostructures (THURSDAY 21 October, Hall 10, 13.30-15.00, poster section)

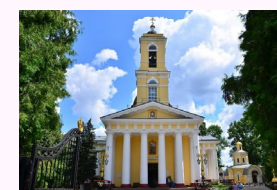
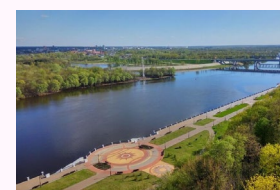
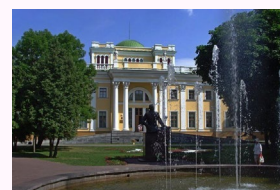
Aushev I. Y.

[Report 51:](#) Simulation of laser splitting of bilayer structures made of silicon wafers and glass substrates (THURSDAY 21 October, Hall 3, 10.00-13.00)
[Report 52:](#) The use of artificial neural networks for determining the parameters of laser processing of fused quartz (THURSDAY 21 October, Hall 3, 10.00-13.00)
[Report 54:](#) Characterization of laser welding of steel 30XГCH2A by combining artificial neural networks and finite element method
(THURSDAY 21 October, Hall 3, 10.00-13.00)

Avdeeva E. V.

[Report 4:](#) Application of additive technology to create universal carriers of cellular structures (WEDNESDAY 20 October, Hall 4, 13.30-15.00, poster section)





Ayvazyan G. Y.

Report 41: Characteristics of nanocomposite sol-gel films on black silicon surface (THURSDAY 21 October, Hall 11, 13.30-15.00, poster section)

Azhagar A.

Report 23: Effects of process parameters on the dissimilar friction stir welded joints between aluminum alloy and polycarbonate (WEDNESDAY 20 October, Hall 6, 13.30-15.00, poster section)

Bakhmetyev V. V.

Report 24: Research of morphology and luminescence of particles based on yttrium fluorides for medical usage (WEDNESDAY 20 October, Hall 7, 13.30-15.00, poster section)

Balabanov S. V.

Report 33: Isotropy mechanical properties products with geometry triple periodic minimal surfaces (TPMS) (THURSDAY 21 October, Hall 1, 10.00-13.00)
Report 36: Impact of modeling method on geometry and mechanical properties of samples with TPMS structure (THURSDAY 21 October, Hall 1, 10.00-13.00)
Report 56: Development of material for 3D printing based on thermoplastic elastomer (THURSDAY 21 October, Hall 3, 10.00-13.00)

Balmakou A.

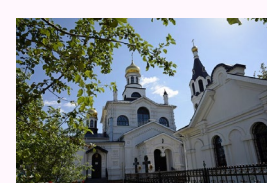
Report 48: Modeling a three-spike absorber in the range 9-13 GHz (THURSDAY 21 October, Hall 1, 10.00-13.00)

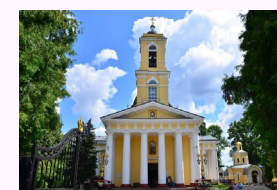
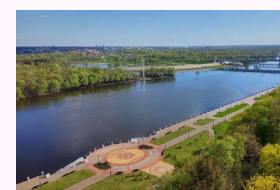
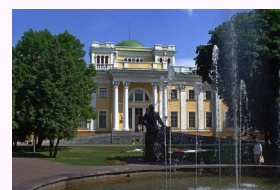
Bayevich G. A.

Report 54: Characterization of laser welding of steel 30XГCH2A by combining artificial neural networks and finite element method (THURSDAY 21 October, Hall 3, 10.00-13.00)

Becker M.

Report 5: Comparison and selection of the greenhouse gas accounting method for a model region in Germany (WEDNESDAY 20 October, Hall 5, 13.30-15.00, Poster section)





Bekarevich R.

[Report 37:](#) Mechanism of double-step conversion reaction in nanostructured tungsten trioxide anode for Li-Ion batteries
(THURSDAY 21 October, Hall 1, 10.00-13.00)

Berger M.

[Report 5:](#) Comparison and selection of the greenhouse gas accounting method for a model region in Germany
(WEDNESDAY 20 October, Hall 5, 13.30-15.00, Poster section)

Besleaga A.

[Report 62:](#) Atomic force spectroscopy experiments with amino-functionalized silicon AFM tips and samples
(WEDNESDAY 20 October, Hall 13, 13.30-15.00, poster section)

Bîrleanu E.

[Report 73:](#) Oxidation and stability of polymers treated by atmospheric-pressure plasma (WEDNESDAY 20 October, Hall 3, 11.00-13.00)

Blajan M. G.

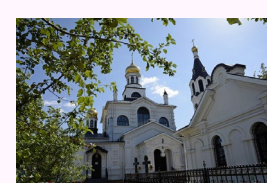
[Report 71:](#) The physicochemical/electrical properties of plasma activated medium by dielectric barrier discharge microplasma
(WEDNESDAY 20 October, Hall 3, 11.00-13.00)

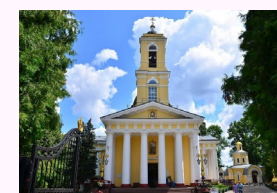
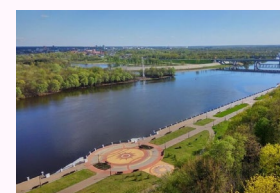
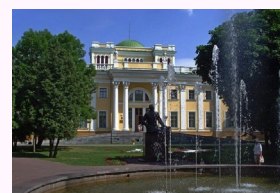
Bogdanov S. P.

[Report 27:](#) The role of the dispersed composition of the diamond matrix in the preparation of a composite by infiltration with molten silicon
(WEDNESDAY 20 October, Hall 1, 11.00-13.00)
[Report 28:](#) Digital materials science (WEDNESDAY 20 October, Hall 1, 11.00-13.00)

Borcia C.

[Report 34:](#) Behavior of electron-beam irradiated polyethylene and polystyrene (THURSDAY 21 October, Hall 1, 10.00-13.00)





Borcia G.

[Report 34:](#) Behavior of electron-beam irradiated polyethylene and polystyrene (THURSDAY 21 October, Hall 1, 10.00-13.00)
[Report 73:](#) Oxidation and stability of polymers treated by atmospheric-pressure plasma (WEDNESDAY 20 October, Hall 3, 11.00-13.00)

Buzhan A. V.

[Report 78:](#) Green functions of relativistic quasipotential equations for complex values of energy (FRIDAY 22 October, Hall 1, 10.00-12.00)

Calistru A. E.

[Report 6:](#) Evaluation of heavy metal contamination in mytilus sp. shells (WEDNESDAY 20 October, Hall 2, 11.00-13.00)

Caponetti E.

[Report 47:](#) Discovering the Sicilian byzantine icons through a combination of imaging and spectroscopic techniques (THURSDAY 21 October, Hall 2, 10.00-13.00)

Chekuryaev A.G.

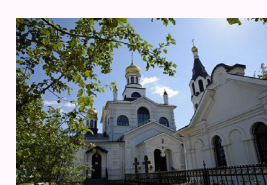
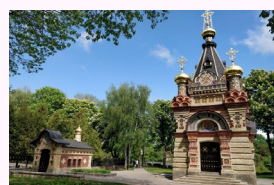
[Report 28:](#) Digital materials science (WEDNESDAY 20 October, Hall 1, 11.00-13.00)

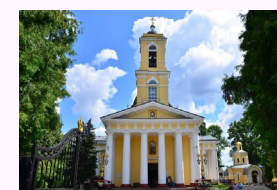
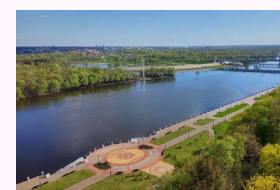
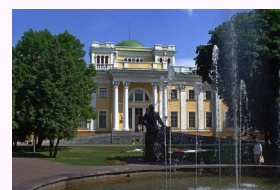
Chirco G.

[Report 47:](#) Discovering the Sicilian byzantine icons through a combination of imaging and spectroscopic techniques (THURSDAY 21 October, Hall 2, 10.00-13.00)

Ciaramitaro V.

[Report 47:](#) Discovering the Sicilian byzantine icons through a combination of imaging and spectroscopic techniques (THURSDAY 21 October, Hall 2, 10.00-13.00)





Ciobanu A.

[Report 66:](#) Photocatalytic activity and wettability of TiO_2 nanotube arrays coupled with WO_3 and ZnO (WEDNESDAY 20 October, Hall 3, 11.00-13.00)

Ciolan M. A.

[Report 6:](#) Evaluation of heavy metal contamination in mytilus sp. shells (WEDNESDAY 20 October, Hall 2, 11.00-13.00)

Costin C.

[Report 72:](#) Velocity distribution functions at plasma boundary (WEDNESDAY 20 October, Hall 3, 11.00-13.00)

Creanga D.

[Report 3:](#) The proton beam influence on the sensitivity of wheat plantlets to AgNP pollution-preliminary results (WEDNESDAY 20 October, Hall 2, 11.00-13.00)

Danilchenko K. D.

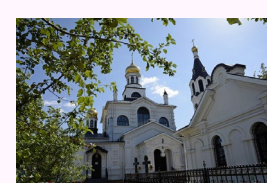
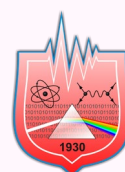
[Report 42:](#) AFM topography of $\text{ZnO}_x\text{:MgO}$ nanocomposite sol-gel films on the surface of silicon (THURSDAY 21 October, Hall 12, 13.30-15.00, poster section)

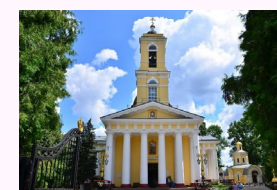
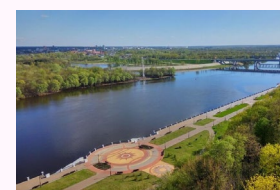
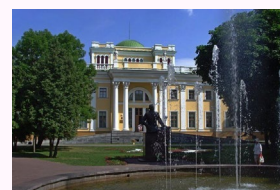
Dobromir M.

[Report 43:](#) Sol-gel synthesis TiO_2 nanotubes based on ZnO nanorods, for use in solar cells (THURSDAY 21 October, Hall 1, 10.00-13.00)
[Report 66:](#) Photocatalytic activity and wettability of TiO_2 nanotube arrays coupled with WO_3 and ZnO (WEDNESDAY 20 October, Hall 3, 11.00-13.00)
[Report 67:](#) Two-steps formation of ZnO -loaded TiO_2 nanotube array films with enhanced photocatalytic performance (WEDNESDAY 20 October, Hall 3, 11.00-13.00)

Dolgin A. S.

[Report 27:](#) The role of the dispersed composition of the diamond matrix in the preparation of a composite by infiltration with molten silicon (WEDNESDAY 20 October, Hall 1, 11.00-13.00)





Dorokhina A. M.

Report 24: Research of morphology and luminescence of particles based on yttrium fluorides for medical usage
(WEDNESDAY 20 October, Hall 7, 13.30-15.00, poster section)

Dovydenko E. M.

Report 4: Application of additive technology to create universal carriers of cellular structures (WEDNESDAY 20 October, Hall 4, 13.30-15.00, poster section)

Emelyanov V. A.

Report 53: Optimization of quartz glass laser polishing parameters using the computational experiment planning method
(THURSDAY 21 October, Hall 3, 10.00-13.00)

Faniayeu I. A.

Report 50: Optical chirality enhancement with dielectric metasurfaces (THURSDAY 21 October, Hall 15, 13.30-15.00, poster section)

Fanyaev I. A.

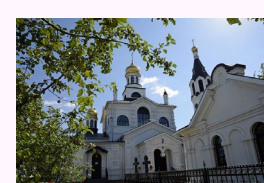
Report 50: Optical chirality enhancement with dielectric metasurfaces (THURSDAY 21 October, Hall 15, 13.30-15.00, poster section)

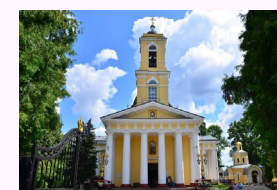
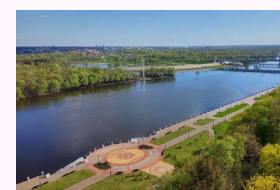
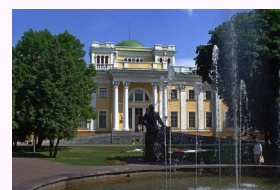
Fedosenko N. N.

Report 29: Structure and properties of metal-carbon a-C coatings alloyed with Ti, Zr and Al with a high concentration
(WEDNESDAY 20 October, Hall 9, 13.30-15.00, poster section)

Fedosenko-Becker T. N.

Report 5: Comparison and selection of the greenhouse gas accounting method for a model region in Germany
(WEDNESDAY 20 October, Hall 5, 13.30-15.00, Poster section)





Fesenko O.

Report 64: Raman investigation of multiferroic BiFeO_3 and $\text{Bi}_{1-x}\text{Sm}_x\text{FeO}_3$ materials synthesized by the sol-gel method
(WEDNESDAY 20 October, Hall 14, 13.30-15.00, Poster section)

Filippov V. V.

Report 44: NiO and NiO:Al films for solar cells: a compromise between electrical conductivity and transparency
(THURSDAY 21 October, Hall 13, 13.30-15.00, poster section)

Filippovich L. V.

Report 30: Polyaniline-based food quality markers (WEDNESDAY 20 October, Hall 1, 11.00-13.00)

Firmansyah T.

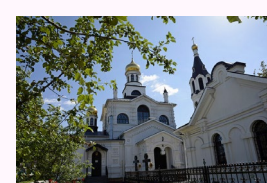
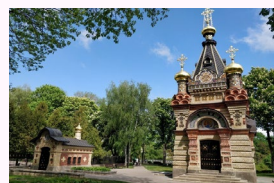
Report 61: Localized surface plasmon resonance liquid sensors based on array gold nanoparticles fabricated on 36XY-LiTaO_3 substrate
(WEDNESDAY 20 October, Hall 12, 13.30-15.00, Poster section)

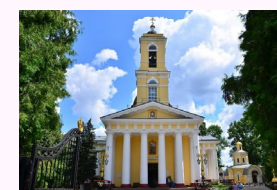
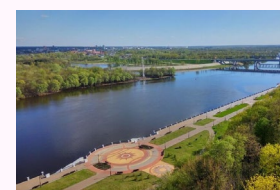
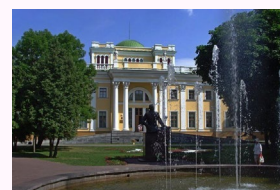
Gaishun V. E.

Report 41: Characteristics of nanocomposite sol-gel films on black silicon surface (THURSDAY 21 October, Hall 11, 13.30-15.00, poster section)
Report 44: NiO and NiO:Al films for solar cells: a compromise between electrical conductivity and transparency
(THURSDAY 21 October, Hall 13, 13.30-15.00, poster section)
Report 46: Development of sapphire-like glass by sol-gel technology (THURSDAY 21 October, Hall 1, 10.00-13.00)
Report 64: Raman investigation of multiferroic BiFeO_3 and $\text{Bi}_{1-x}\text{Sm}_x\text{FeO}_3$ materials synthesized by the sol-gel method
(WEDNESDAY 20 October, Hall 14, 13.30-15.00, Poster section)

Gnatyuk V. A.

Report 26: Investigation of the convection effect on the inclusion motion in thermally stressed crystals
(WEDNESDAY 20 October, Hall 8, 13.30-15.00, poster section)





Gomidze N. Kh.

Report 14: 3D Fluorescence spectroscopy of liquid media via internal reference method (THURSDAY 21 October, Hall 2, 10.00-13.00)

Grishechkin Yu. A.

Report 76: Numerical solution of the two-dimensional Logunov-Tavkhelidze equation with the sum of two separable potentials in the momentum representation (FRIDAY 22 October, Hall 1, 10.00-12.00)

Grishechkina A. A.

Report 77: Partial two-particle equations in the relativistic configurational representation for scattering p-states in the case of a superposition of two δ -function potentials (FRIDAY 22 October, Hall 1, 10.00-12.00)

Hakhoyan L. A.

Report 41: Characteristics of nanocomposite sol-gel films on black silicon surface (THURSDAY 21 October, Hall 11, 13.30-15.00, poster section)

Hara K.

Report 25: One-step microwave synthesis of Eu^{2+} -doped silicate and chlorinesilicate phosphors mixture for application in light sources (WEDNESDAY 20 October, Hall 1, 11.00-13.00)

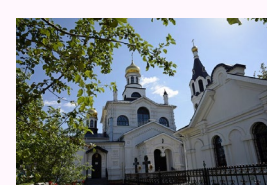
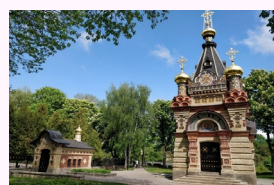
Harish S.

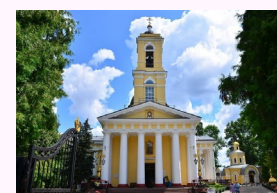
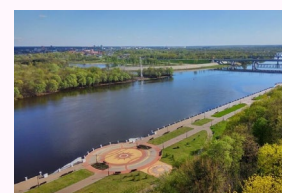
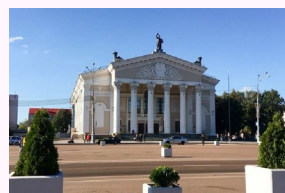
Report 38: Enhancing the seebeck coefficient of Zn-doped MoS_2 grown over carbon fabrics via band engineering (WEDNESDAY 20 October, Hall 11, 13.30-15.00, poster section)

Report 40: Investigation on influence of Cu doping on thermoelectric performance of tin-selenide-based nanostructures (THURSDAY 21 October, Hall 10, 13.30-15.00, poster section)

Hashimoto K.

Report 7: In vivo measurement of dielectric properties of human skin using attenuated total reflection terahertz time domain spectroscopy (WEDNESDAY 20 October, Hall 2, 11.00-13.00)





Hashimoto M.

[Report 12:](#) Evaluation of radiation detection characteristics by $\alpha\text{-Ga}_2\text{O}_3$ (THURSDAY 21 October, Hall 2, 10.00-13.00)

Hatescu I.

[Report 34:](#) Behavior of electron-beam irradiated polyethylene and polystyrene (THURSDAY 21 October, Hall 1, 10.00-13.00)

Hayakawa K.

[Report 23:](#) Effects of process parameters on the dissimilar friction stir welded joints between aluminum alloy and polycarbonate (WEDNESDAY 20 October, Hall 6, 13.30-15.00, poster section)

Hayakawa Y.

[Report 39:](#) Effect of Ag substitution on enhancing the thermoelectric performance of nanostructured SnSe (THURSDAY 21 October, Hall 1, 10.00-13.00)

Hiroto T.

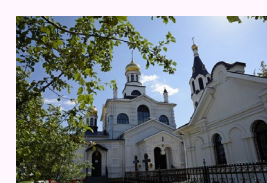
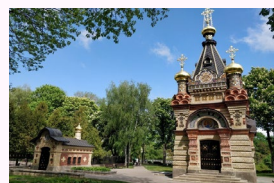
[Report 37:](#) Mechanism of double-step conversion reaction in nanostructured tungsten trioxide anode for Li-Ion batteries (THURSDAY 21 October, Hall 1, 10.00-13.00)

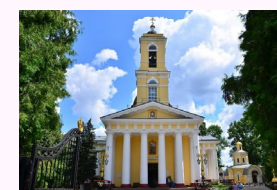
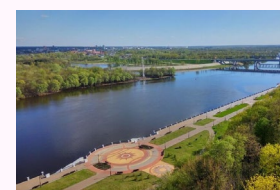
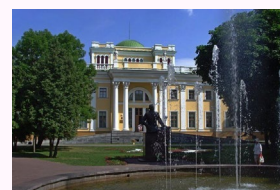
Hitomi K.

[Report 75:](#) Spatial resolution of X-ray imaging using 80 μm pitch TlBr detector (FRIDAY 22 October, Hall 1, 10.00-12.00)

Honda T.

[Report 12:](#) Evaluation of radiation detection characteristics by $\alpha\text{-Ga}_2\text{O}_3$ (THURSDAY 21 October, Hall 2, 10.00-13.00)





Hreniak D.

[Report 47:](#) Discovering the Sicilian byzantine icons through a combination of imaging and spectroscopic techniques
 (THURSDAY 21 October, Hall 2, 10.00-13.00)

Ignatenko O. V.

[Report 46:](#) Development of sapphire-like glass by sol-gel technology (THURSDAY 21 October, Hall 1, 10.00-13.00)

Ignatovich J. V.

[Report 30:](#) Polyaniline-based food quality markers (WEDNESDAY 20 October, Hall 1, 11.00-13.00)

Ikeda H.

[Report 38:](#) Enhancing the seebeck coefficient of Zn-doped MoS₂ grown over carbon fabrics via band engineering
 (WEDNESDAY 20 October, Hall 11, 13.30-15.00, poster section)
[Report 39:](#) Effect of Ag substitution on enhancing the thermoelectric performance of nanostructured SnSe (THURSDAY 21 October, Hall 1, 10.00-13.00)
[Report 40:](#) Investigation on influence of Cu doping on thermoelectric performance of tin-selenide-based nanostructures
 (THURSDAY 21 October, Hall 10, 13.30-15.00, poster section)

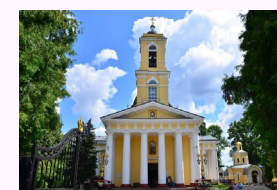
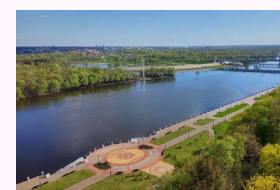
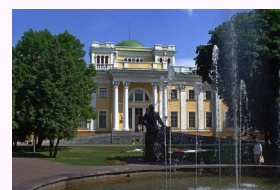
Ishiguro K.

[Report 45:](#) The effect of SiO₂ content rate in simulated lunar regolith on ablation plume temperature and the feasibility assessment of Al₂O₃ reduction
 (THURSDAY 21 October, Hall 14, 13.30-15.00, poster section)

Iwatsuki Y.

[Report 9:](#) Probing of deep states by band-to-band tunneling in nanoscale silicon-on-insulator Esaki diodes (THURSDAY 21 October, Hall 2, 10.00-13.00)





Jayavel R.

[Report 39:](#) Effect of Ag substitution on enhancing the thermoelectric performance of nanostructured SnSe (THURSDAY 21 October, Hall 1, 10.00-13.00)

Jinxing Cao

[Report 69:](#) Studies of magnesium – hydroxyapatite micro/nano film for drug sustained release (WEDNESDAY 20 October, Hall 3, 11.00-13.00)

Jialin Fang

[Report 29:](#) Structure and properties of metal-carbon a-C coatings alloyed with Ti, Zr and Al with a high concentration (WEDNESDAY 20 October, Hall 9, 13.30-15.00, poster section)

Jiang X.-H.

[Report 29:](#) Structure and properties of metal-carbon a-C coatings alloyed with Ti, Zr and Al with a high concentration (WEDNESDAY 20 October, Hall 9, 13.30-15.00, poster section)

Jitareanu G.

[Report 6:](#) Evaluation of heavy metal contamination in mytilus sp. Shells (WEDNESDAY 20 October, Hall 2, 11.00-13.00)

Kalaiarasan K.

[Report 39:](#) Effect of Ag substitution on enhancing the thermoelectric performance of nanostructured SnSe (THURSDAY 21 October, Hall 1, 10.00-13.00)

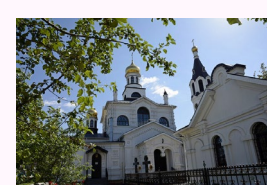
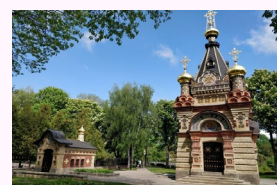
Kapshai V. N.

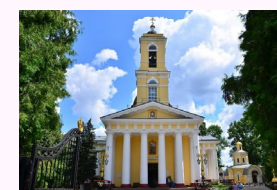
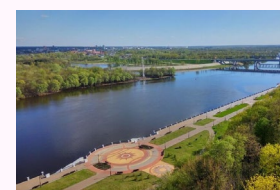
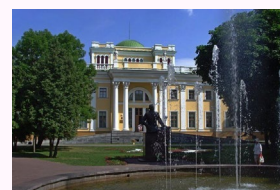
[Report 77:](#) Partial two-particle equations in the relativistic configurational representation for scattering p-states in the case of a superposition of two δ - function potentials (FRIDAY 22 October, Hall 1, 10.00-12.00)

[Report 78:](#) Green functions of relativistic quasipotential equations for complex values of energy (FRIDAY 22 October, Hall 1, 10.00-12.00)

[Report 79:](#) Analysis of the spatial distribution of the second-harmonic radiation generated in a thin surface layer of a spheroidal dielectric particle (FRIDAY 22 October, Hall 1, 10.00-12.00)

[Report 80:](#) Maxima of the power density of the second-harmonic generation from a linear structure of long cylindrical dielectric particles (FRIDAY 22 October, Hall 1, 10.00-12.00)





Kase H.

Report 21: Applications for effective representation of imaging with X-ray CT (THURSDAY 21 October, Hall 9, 13.30-15.00, poster section)
Report 75: Spatial resolution of X-ray imaging using 80µm pitch TlBr detector (FRIDAY 22 October, Hall 1, 10.00-12.00)

Kashko I. A.

Report 44: NiO and NiO:Al films for solar cells: a compromise between electrical conductivity and transparency
(THURSDAY 21 October, Hall 13, 13.30-15.00, poster section)

Kawauchi T.

Report 70: High power terahertz wave emission using DAST crystal (WEDNESDAY 20 October, Hall 17, 13.30-15.00, Poster section)

Keskinova M. V.

Report 25: One-step microwave synthesis of Eu²⁺-doped silicate and chlorinesilicate phosphors mixture for application in light sources
(WEDNESDAY 20 October, Hall 1, 11.00-13.00)

Khakhomov S.

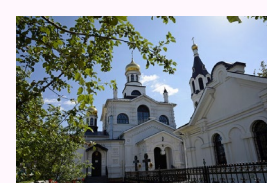
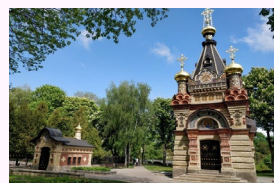
Report 48: Modeling a three-spike absorber in the range 9-13 GHz (THURSDAY 21 October, Hall 1, 10.00-13.00)
Report 49: Production and experimental study of a weakly reflecting absorbing metamaterial based on planar spirals in the microwave range
(THURSDAY 21 October, Hall 1, 10.00-13.00)
Report 64: Raman investigation of multiferroic BiFeO₃ and Bi_{1-x}Sm_xFeO₃ materials synthesized by the sol-gel method
(WEDNESDAY 20 October, Hall 14, 13.30-15.00, Poster section)

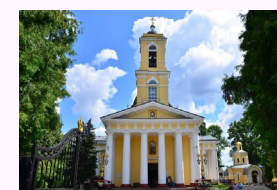
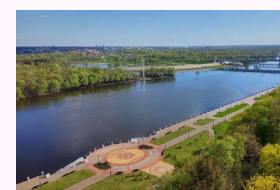
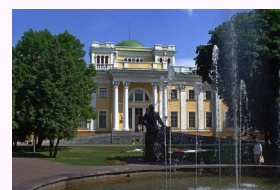
Khajishvili M. R.

Report 14: 3D Fluorescence spectroscopy of liquid media via internal reference method (THURSDAY 21 October, Hall 2, 10.00-13.00)

Kiselev D. A.

Report 65: Piezoelectric properties of SrBi₂(Ta_xNb_{1-x})₂O₉ thin films synthesized by the sol-gel method
(WEDNESDAY 20 October, Hall 15, 13.30-15.00, Poster section)





Kobayashi R.

[Report 57:](#) Investigation of the effect of observation window on the sensitivity enhancement in the multi-pass cell outside the expansion wave tube chamber (THURSDAY 21 October, Hall 16, 13.30-15.00, poster section)

Koike A.

[Report 75:](#) Spatial resolution of X-ray imaging using 80μm pitch TlBr detector (FRIDAY 22 October, Hall 1, 10.00-12.00)

Kominami H.

[Report 24:](#) Research of morphology and luminescence of particles based on yttrium fluorides for medical usage (WEDNESDAY 20 October, Hall 7, 13.30-15.00, poster section)

Kondoh J.

[Report 13:](#) Transportation and measurement of droplet using surface acoustic wave for digital microfluidic system application (THURSDAY 21 October, Hall 2, 10.00-13.00)
[Report 61:](#) Localized surface plasmon resonance liquid sensors based on array gold nanoparticles fabricated on 36XY-LiTaO₃ substrate (WEDNESDAY 20 October, Hall 12, 13.30-15.00, Poster section)

Konrad-Soare C. T.

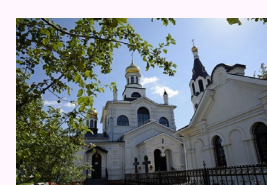
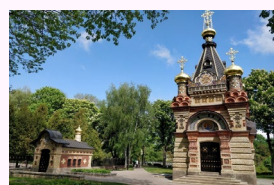
[Report 66:](#) Photocatalytic activity and wettability of TiO₂ nanotube arrays coupled with WO₃ and ZnO (WEDNESDAY 20 October, Hall 3, 11.00-13.00)
[Report 67:](#) Two-steps formation of ZnO-loaded TiO₂ nanotube array films with enhanced photocatalytic performance (WEDNESDAY 20 October, Hall 3, 11.00-13.00)

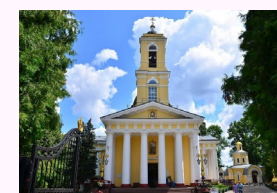
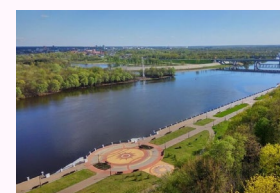
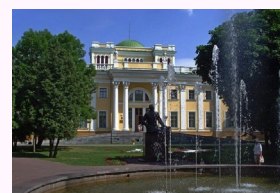
Kontsevaya I. I.

[Report 31:](#) Vacuum coatings based on miramistin and their biological properties (WEDNESDAY 20 October, Hall 1, 11.00-13.00)

Kosenok Ya. A.

[Report 46:](#) Development of sapphire-like glass by sol-gel technology (THURSDAY 21 October, Hall 1, 10.00-13.00)
[Report 43:](#) Sol-gel synthesis TiO₂ nanotubes based on ZnO nanorods, for use in solar cells (THURSDAY 21 October, Hall 1, 10.00-13.00)





Koshevaya K. S.

Report 33: Isotropy mechanical properties products with geometry triple periodic minimal surfaces (TPMS) (THURSDAY 21 October, Hall 1, 10.00-13.00)
Report 36: Impact of modeling method on geometry and mechanical properties of samples with TPMS structure (THURSDAY 21 October, Hall 1, 10.00-13.00)

Košťál I.

Report 19: A parallelization of instance methods of a .NET application that search for required structured data stored in a skip list
(THURSDAY 21 October, Hall 7, 13.30-15.00, poster section)

Kovalenko D. L.

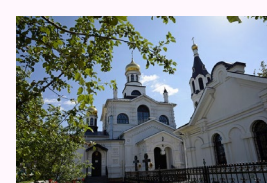
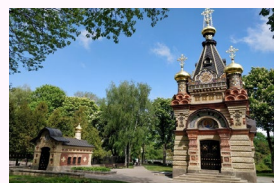
Report 41: Characteristics of nanocomposite sol-gel films on black silicon surface (THURSDAY 21 October, Hall 11, 13.30-15.00, poster section)
Report 43: Sol-gel synthesis TiO_2 nanotubes based on ZnO nanorods, for use in solar cells (THURSDAY 21 October, Hall 1, 10.00-13.00)
Report 44: NiO and NiO:Al films for solar cells: a compromise between electrical conductivity and transparency
(THURSDAY 21 October, Hall 13, 13.30-15.00, poster section)
Report 46: Development of sapphire-like glass by sol-gel technology (THURSDAY 21 October, Hall 1, 10.00-13.00)
Report 64: Raman investigation of multiferroic BiFeO_3 and $\text{Bi}_{1-x}\text{Sm}_x\text{FeO}_3$ materials synthesized by the sol-gel method
(WEDNESDAY 20 October, Hall 14, 13.30-15.00, Poster section)
Report 67: Two-steps formation of ZnO-loaded TiO_2 nanotube array films with enhanced photocatalytic performance
(WEDNESDAY 20 October, Hall 3, 11.00-13.00)

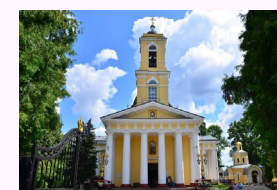
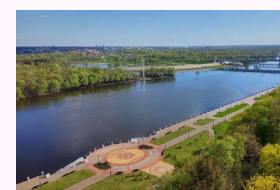
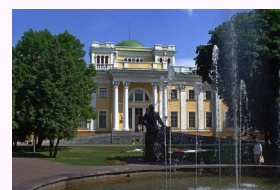
Koyama C.

Report 70: High power terahertz wave emission using DAST crystal (WEDNESDAY 20 October, Hall 17, 13.30-15.00, Poster section)

Kravchenko A.

Report 49: Production and experimental study of a weakly reflecting absorbing metamaterial based on planar spirals in the microwave range
(THURSDAY 21 October, Hall 1, 10.00-13.00)





Kravets V. A.

[Report 32:](#) **Synthesis of scintillating glass materials containing yttrium niobate crystallites activated with terbium ions**
 (WEDNESDAY 20 October, Hall 1, 11.00-13.00)

Kristof J.

[Report 71:](#) **The physicochemical/electrical properties of plasma activated medium by dielectric barrier discharge microplasma**
 (WEDNESDAY 20 October, Hall 3, 11.00-13.00)

Kulesh E. A.

[Report 29:](#) **Structure and properties of metal-carbon a-C coatings alloyed with Ti, Zr and Al with a high concentration**
 (WEDNESDAY 20 October, Hall 9, 13.30-15.00, poster section)

Kulyk O. P.

[Report 26:](#) **Investigation of the convection effect on the inclusion motion in thermally stressed crystals**
 (WEDNESDAY 20 October, Hall 8, 13.30-15.00, poster section)

Kuznetsov P.A.

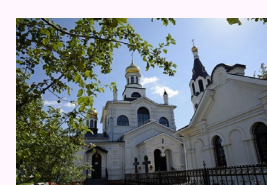
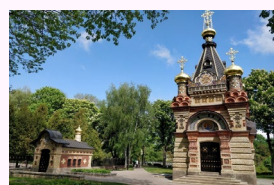
[Report 28:](#) **Digital Materials Science** (WEDNESDAY 20 October, Hall 1, 11.00-13.00)

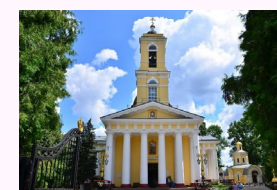
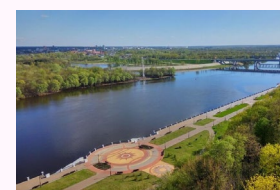
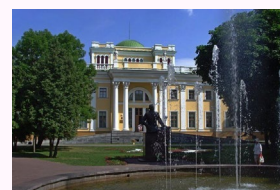
Laznev K. V.

[Report 4:](#) **Application of additive technology to create universal carriers of cellular structures** (WEDNESDAY 20 October, Hall 4, 13.30-15.00, poster section)

Leibgam V.

[Report 27:](#) **The role of the dispersed composition of the diamond matrix in the preparation of a composite by infiltration with molten silicon**
 (WEDNESDAY 20 October, Hall 1, 11.00-13.00)





Les A.

Report 3: The proton beam influence on the sensitivity of wheat plantlets to AgNP pollution-preliminary results (WEDNESDAY 20 October, Hall 2, 11.00-13.00)

Lo Re G.

Report 47: Discovering the Sicilian byzantine icons through a combination of imaging and spectroscopic techniques (THURSDAY 21 October, Hall 2, 10.00-13.00)

Luca M.

Report 66: Photocatalytic activity and wettability of TiO_2 nanotube arrays coupled with WO_3 and ZnO (WEDNESDAY 20 October, Hall 3, 11.00-13.00)

Luca D.

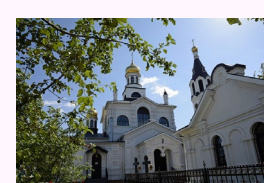
Report 43: Sol-gel synthesis TiO_2 nanotubes based on ZnO nanorods, for use in solar cells (THURSDAY 21 October, Hall 1, 10.00-13.00)
Report 66: Photocatalytic activity and wettability of TiO_2 nanotube arrays coupled with WO_3 and ZnO (WEDNESDAY 20 October, Hall 3, 11.00-13.00)
Report 67: Two-steps formation of ZnO -loaded TiO_2 nanotube array films with enhanced photocatalytic performance (WEDNESDAY 20 October, Hall 3, 11.00-13.00)

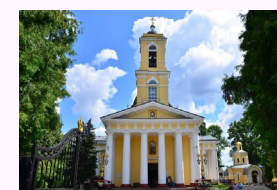
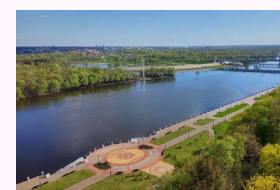
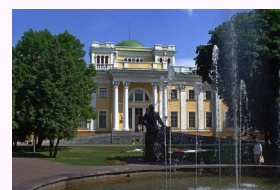
Makogon A. I.

Report 33: Isotropy mechanical properties products with geometry triple periodic minimal surfaces (TPMS) (THURSDAY 21 October, Hall 1, 10.00-13.00)
Report 36: Impact of modeling method on geometry and mechanical properties of samples with TPMS structure (THURSDAY 21 October, Hall 1, 10.00-13.00)
Report 55: Investigation of acoustic wave propagation in complex geometry (THURSDAY 21 October, Hall 3, 10.00-13.00)

Malyutina-Bronskaya V.V.

Report 42: AFM topography of $\text{ZnO}_x:\text{MgO}$ nanocomposite sol-gel films on the surface of silicon (THURSDAY 21 October, Hall 12, 13.30-15.00, poster section)





Masuzawa T.

Report 74: Diamond radiation detector with built-in boron-doped neutron converter layer (FRIDAY 22 October, Hall 1, 10.00-12.00)

Matsui M.

Report 45: The effect of SiO₂ content rate in simulated lunar regolith on ablation plume temperature and the feasibility assessment of Al₂O₃ reduction (THURSDAY 21 October, Hall 14, 13.30-15.00, poster section)

Report 57: Investigation of the effect of observation window on the sensitivity enhancement in the multi-pass cell outside the expansion wave tube chamber (THURSDAY 21 October, Hall 16, 13.30-15.00, poster section)

Matsushita Y.

Report 37: Mechanism of double-step conversion reaction in nanostructured tungsten trioxide anode for Li-Ion batteries (THURSDAY 21 October, Hall 1, 10.00-13.00)

Maximenko A. V.

Report 54: Characterization of laser welding of steel 30XГCH2A by combining artificial neural networks and finite element method (THURSDAY 21 October, Hall 3, 10.00-13.00)

Midiri M.

Report 47: Discovering the Sicilian byzantine icons through a combination of imaging and spectroscopic techniques (THURSDAY 21 October, Hall 2, 10.00-13.00)

Mihaila I.

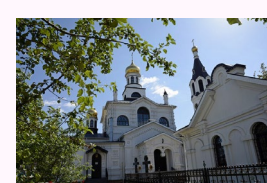
Report 73: Oxidation and stability of polymers treated by atmospheric-pressure plasma (WEDNESDAY 20 October, Hall 3, 11.00-13.00)

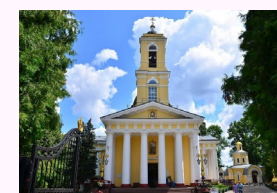
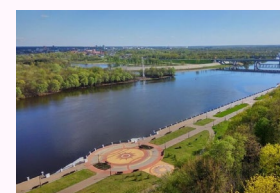
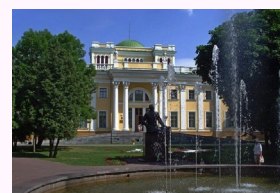
Mimura H.

Report 16: High-performance and low-voltage current sense-amplifier using GAA-CNTFET with different chirality and channel (THURSDAY 21 October, Hall 5, 13.30-15.00, poster section)

Report 17: Theoretical study of the impact of a donor-acceptor pair on tunneling current in Si nanodiodes (THURSDAY 21 October, Hall 6, 13.30-15.00, poster section)

Report 74: Diamond radiation detector with built-in boron-doped neutron converter layer (FRIDAY 22 October, Hall 1, 10.00-12.00)





Miron L. D.

Report 6: Evaluation of heavy metal contamination in mytilus sp. shells (WEDNESDAY 20 October, Hall 2, 11.00-13.00)

Mitsuyoshi R.

Report 13: Transportation and measurement of droplet using surface acoustic wave for digital microfluidic system application
(THURSDAY 21 October, Hall 2, 10.00-13.00)

Miyake T.

Report 74: Diamond radiation detector with built-in boron-doped neutron converter layer (FRIDAY 22 October, Hall 1, 10.00-12.00)

Molokanov A.

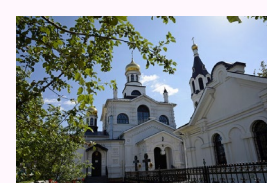
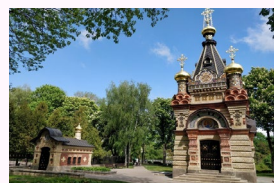
Report 3: The proton beam influence on the sensitivity of wheat plantlets to AgNP pollution-preliminary results (WEDNESDAY 20 October, Hall 2, 11.00-13.00)

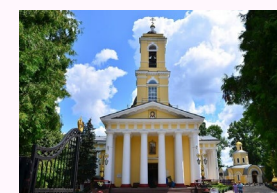
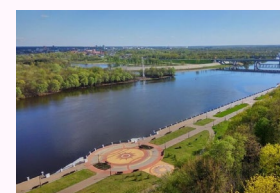
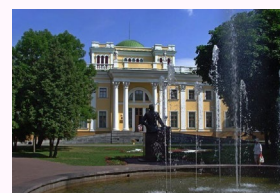
Moraru D.

Report 9: Probing of deep states by band-to-band tunneling in nanoscale silicon-on-insulator Esaki diodes (THURSDAY 21 October, Hall 2, 10.00-13.00)
Report 15: First-principles study of bandgap electronic states under electric field in silicon nanowires with discrete dopants
(THURSDAY 21 October, Hall 4, 13.30-15.00, poster section)
Report 17: Theoretical study of the impact of a donor-acceptor pair on tunneling current in Si nanodiodes
(THURSDAY 21 October, Hall 6, 13.30-15.00, poster section)

Morii H.

Report 24: Research of morphology and luminescence of particles based on yttrium fluorides for medical usage
(WEDNESDAY 20 October, Hall 7, 13.30-15.00, poster section)
Report 75: Spatial resolution of X-ray imaging using 80µm pitch TlBr detector (FRIDAY 22 October, Hall 1, 10.00-12.00)





Mosavi A.

Report 1: Investigating urban sustainability by emphasizing on the approaches for reducing fuel consumption using intelligent transportation system (WEDNESDAY 20 October, Hall 2, 11.00-13.00)
Report 2: Environmental risk management by achieving sustainable development goals in architecture and urban engineering (WEDNESDAY 20 October, Hall 2, 11.00-13.00)
Report 20: Deep learning applications for COVID-19: a brief review (THURSDAY 21 October, Hall 8, 13.30-15.00, poster section)

Moskvichyov M. I.

Report 32: Synthesis of scintillating glass materials containing yttrium niobate crystallites activated with terbium ions (WEDNESDAY 20 October, Hall 1, 11.00-13.00)

Motrescu I.

Report 6: Evaluation of heavy metal contamination in mytilus sp. shells (WEDNESDAY 20 October, Hall 2, 11.00-13.00)

Myshkovets V. N.

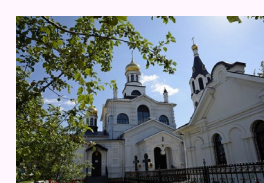
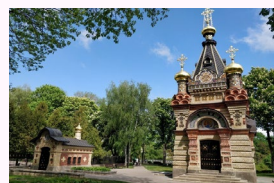
Report 54: Characterization of laser welding of steel 30XГCH2A by combining artificial neural networks and finite element method (THURSDAY 21 October, Hall 3, 10.00-13.00)

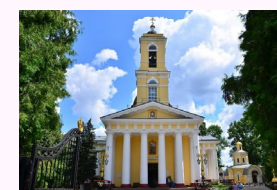
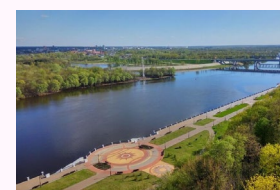
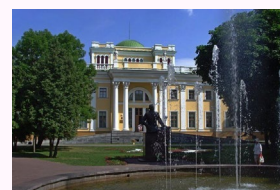
Nakagawa H.

Report 12: Evaluation of radiation detection characteristics by $\alpha\text{-Ga}_2\text{O}_3$ (THURSDAY 21 October, Hall 2, 10.00-13.00)
Report 74: Diamond radiation detector with built-in boron-doped neutron converter layer (FRIDAY 22 October, Hall 1, 10.00-12.00)

Nakano T.

Report 12: Evaluation of radiation detection characteristics by $\alpha\text{-Ga}_2\text{O}_3$ (THURSDAY 21 October, Hall 2, 10.00-13.00)
Report 74: Diamond radiation detector with built-in boron-doped neutron converter layer (FRIDAY 22 October, Hall 1, 10.00-12.00)





Navaneethan M.

Report 38: Enhancing the seebeck coefficient of Zn-doped MoS₂ grown over carbon fabrics via band engineering

(WEDNESDAY 20 October, Hall 11, 13.30-15.00, poster section)

Report 40: Investigation on influence of Cu doping on thermoelectric performance of tin-selenide-based nanostructures

(THURSDAY 21 October, Hall 10, 13.30-15.00, poster section)

Neo Y.

Report 17: Theoretical study of the impact of a donor-acceptor pair on tunneling current in Si nanodiodes

(THURSDAY 21 October, Hall 6, 13.30-15.00, poster section)

Nikiforov D. I.

Report 56: Development of material for 3D printing based on thermoplastic elastomer (THURSDAY 21 October, Hall 3, 10.00-13.00)

Nikitjuk Yu. V.

Report 22: The use of design automation tools in training young specialists in radio electronics (THURSDAY 21 October, Hall 3, 10.00-13.00)

Report 51: Simulation of laser splitting of bilayer structures made of silicon wafers and glass substrates (THURSDAY 21 October, Hall 3, 10.00-13.00)

Report 52: The use of artificial neural networks for determining the parameters of laser processing of fused quartz (THURSDAY 21 October, Hall 3, 10.00-13.00)

Report 53: Optimization of quartz glass laser polishing parameters using the computational experiment planning method

(THURSDAY 21 October, Hall 3, 10.00-13.00)

Report 54: Characterization of laser welding of steel 30XГCH2A by combining artificial neural networks and finite element method

(THURSDAY 21 October, Hall 3, 10.00-13.00)

Nishikawa K.

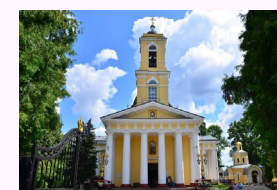
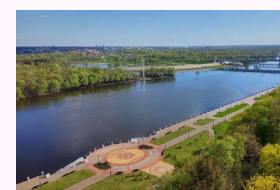
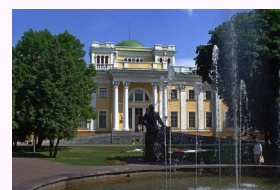
Report 37: Mechanism of double-step conversion reaction in nanostructured tungsten trioxide anode for Li-Ion batteries

(THURSDAY 21 October, Hall 1, 10.00-13.00)

Nogami M.

Report 75: Spatial resolution of X-ray imaging using 80μm pitch TlBr detector (FRIDAY 22 October, Hall 1, 10.00-12.00)





Novik H. A.

[Report 30:](#) Polyaniline-based food quality markers (WEDNESDAY 20 October, Hall 1, 11.00-13.00)

Ohtake G.

[Report 70:](#) High power terahertz wave emission using DAST crystal (WEDNESDAY 20 October, Hall 17, 13.30-15.00, Poster section)

Oishi R.

[Report 45:](#) The effect of SiO_2 content rate in simulated lunar regolith on ablation plume temperature and the feasibility assessment of Al_2O_3 reduction (THURSDAY 21 October, Hall 14, 13.30-15.00, poster section)

Okuyama T.

[Report 71:](#) The physicochemical/electrical properties of plasma activated medium by dielectric barrier discharge microplasma (WEDNESDAY 20 October, Hall 3, 11.00-13.00)

Onuma T.

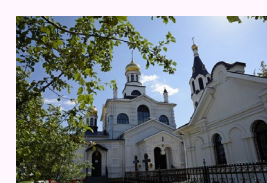
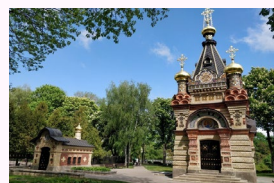
[Report 12:](#) Evaluation of radiation detection characteristics by $\alpha\text{-Ga}_2\text{O}_3$ (THURSDAY 21 October, Hall 2, 10.00-13.00)

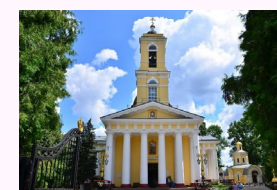
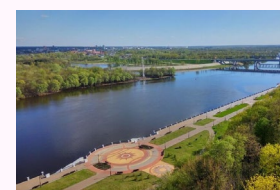
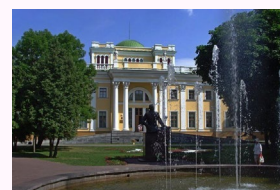
Ota S. R.

[Report 59:](#) Online lesson “Academic English I” for students (THURSDAY 21 October, Hall 17, 13.30-15.00, poster section)

Pandy C.

[Report 17:](#) Theoretical study of the impact of a donor-acceptor pair on tunneling current in Si nanodiodes (THURSDAY 21 October, Hall 6, 13.30-15.00, poster section)





Paulenko A. V.

Report 76: Numerical solution of the two-dimensional Logunov-Tavkhelidze equation with the sum of two separable potentials in the momentum representation (FRIDAY 22 October, Hall 1, 10.00-12.00)

Petkevich A. V.

Report 4: Application of additive technology to create universal carriers of cellular structures (WEDNESDAY 20 October, Hall 4, 13.30-15.00, poster section)

Pilipenko V.A.

Report 42: AFM topography of $\text{ZnO}_x\text{:MgO}$ nanocomposite sol-gel films on the surface of silicon (THURSDAY 21 October, Hall 12, 13.30-15.00, poster section)
Report 65: Piezoelectric properties of $\text{SrBi}_2(\text{Ta}_x\text{Nb}_{1-x})_2\text{O}_9$ thin films synthesized by the sol-gel method (WEDNESDAY 20 October, Hall 15, 13.30-15.00, Poster section)

Piliptsou D. G.

Report 29: Structure and properties of metal-carbon a-C coatings alloyed with Ti, Zr and Al with a high concentration (WEDNESDAY 20 October, Hall 9, 13.30-15.00, poster section)
Report 35: Structure and optical properties of a-C coatings doped with nitrogen and silicon (WEDNESDAY 20 October, Hall 10, 13.30-15.00, poster section)

Pihosh Y.

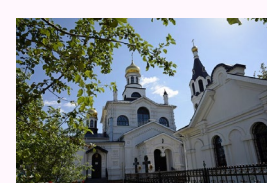
Report 37: Mechanism of double-step conversion reaction in nanostructured tungsten trioxide anode for Li-Ion batteries (THURSDAY 21 October, Hall 1, 10.00-13.00)

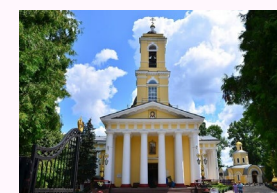
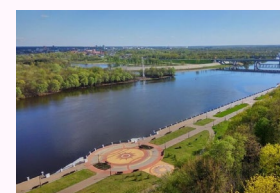
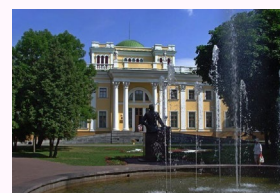
Pobiyaha A. S.

Report 35: Structure and optical properties of a-C coatings doped with nitrogen and silicon (WEDNESDAY 20 October, Hall 10, 13.30-15.00, poster section)
Report 63: Heat treatment effect on the mechanical properties of nanostructured carbon coatings (WEDNESDAY 20 October, Hall 3, 11.00-13.00)

Podshyvalova O. V.

Report 26: Investigation of the convection effect on the inclusion motion in thermally stressed crystals (WEDNESDAY 20 October, Hall 8, 13.30-15.00, poster section)





Prokhorenko V. A.

[Report 52:](#) The use of artificial neural networks for determining the parameters of laser processing of fused quartz (THURSDAY 21 October, Hall 3, 10.00-13.00)

Rahardjo E. T.

[Report 61:](#) Localized surface plasmon resonance liquid sensors based on array gold nanoparticles fabricated on 36XY-LiTaO₃ substrate (WEDNESDAY 20 October, Hall 12, 13.30-15.00, Poster section)

Rajasekaran P.

[Report 39:](#) Effect of Ag substitution on enhancing the thermoelectric performance of nanostructured SnSe (THURSDAY 21 October, Hall 1, 10.00-13.00)

Rakos B.

[Report 10:](#) A fluorescent protein-based AND gate for photon-coupled protein logic (THURSDAY 21 October, Hall 2, 10.00-13.00)

[Report 11:](#) An angle-sensitive, nickel bolometer-based, adaptive infrared pixel antenna (THURSDAY 21 October, Hall 2, 10.00-13.00)

Razmara J.

[Report 20:](#) Deep learning applications for COVID-19: a brief review (THURSDAY 21 October, Hall 8, 13.30-15.00, poster section)

Rituraj R.

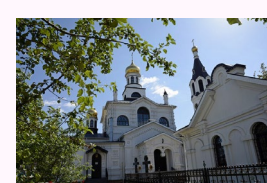
[Report 58:](#) Modeling and optimization of a microgrid for a midrise apartment and industry (THURSDAY 21 October, Hall 3, 10.00-13.00)

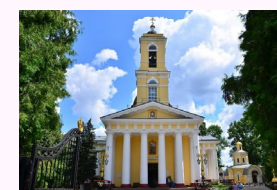
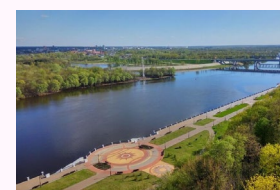
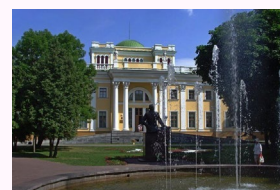
Rogachev A. A.

[Report 4:](#) Application of additive technology to create universal carriers of cellular structures (WEDNESDAY 20 October, Hall 4, 13.30-15.00, poster section)

[Report 30:](#) Polyaniline-based food quality markers (WEDNESDAY 20 October, Hall 1, 11.00-13.00)

[Report 31:](#) Vacuum coatings based on miramistin and their biological properties (WEDNESDAY 20 October, Hall 1, 11.00-13.00)





Rogachev A. V.

Report 29: Structure and properties of metal-carbon a-C coatings alloyed with Ti, Zr and Al with a high concentration

(WEDNESDAY 20 October, Hall 9, 13.30-15.00, poster section)

Report 35: Structure and optical properties of a-C coatings doped with nitrogen and silicon (WEDNESDAY 20 October, Hall 10, 13.30-15.00, poster section)

Report 69: Studies of magnesium – hydroxyapatite micro/nano film for drug sustained release (WEDNESDAY 20 October, Hall 3, 11.00-13.00)

Rudnikov A.S.

Report 35: Structure and optical properties of a-C coatings doped with nitrogen and silicon (WEDNESDAY 20 October, Hall 10, 13.30-15.00, poster section)

Report 63: Heat treatment effect on the mechanical properties of nanostructured carbon coatings (WEDNESDAY 20 October, Hall 3, 11.00-13.00)

Sakai H.

Report 57: Investigation of the effect of observation window on the sensitivity enhancement in the multi-pass cell outside the expansion wave tube chamber (THURSDAY 21 October, Hall 16, 13.30-15.00, poster section)

Sakai K.

Report 23: Effects of process parameters on the dissimilar friction stir welded joints between aluminum alloy and polycarbonate (WEDNESDAY 20 October, Hall 6, 13.30-15.00, poster section)

Sakata H.

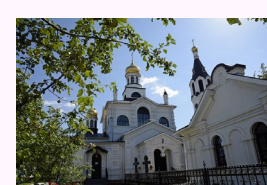
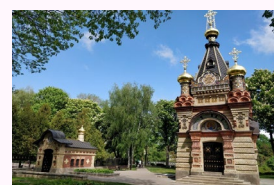
Report 7: In vivo measurement of dielectric properties of human skin using attenuated total reflection terahertz time domain spectroscopy (WEDNESDAY 20 October, Hall 2, 11.00-13.00)

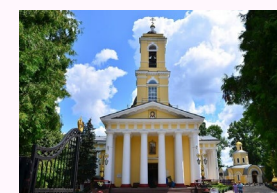
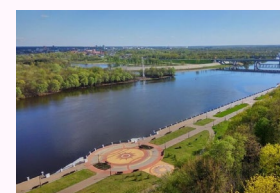
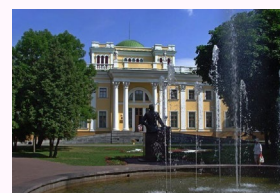
Saladino M. L.

Report 47: Discovering the Sicilian byzantine icons through a combination of imaging and spectroscopic techniques (THURSDAY 21 October, Hall 2, 10.00-13.00)

Samofalov A.

Report 49: Production and experimental study of a weakly reflecting absorbing metamaterial based on planar spirals in the microwave range (THURSDAY 21 October, Hall 1, 10.00-13.00)





Semchenko A. V.

Report 32: Synthesis of scintillating glass materials containing yttrium niobate crystallites activated with terbium ions

(WEDNESDAY 20 October, Hall 1, 11.00-13.00)

Report 41: Characteristics of nanocomposite sol-gel films on black silicon surface (THURSDAY 21 October, Hall 11, 13.30-15.00, poster section)

Report 42: AFM topography of $\text{ZnO}_x\text{:MgO}$ nanocomposite sol-gel films on the surface of silicon (THURSDAY 21 October, Hall 12, 13.30-15.00, poster section)

Report 43: Sol-gel synthesis TiO_2 nanotubes based on ZnO nanorods, for use in solar cells (THURSDAY 21 October, Hall 1, 10.00-13.00)

Report 64: Raman investigation of multiferroic BiFeO_3 and $\text{Bi}_{1-x}\text{Sm}_x\text{FeO}_3$ materials synthesized by the sol-gel method

(WEDNESDAY 20 October, Hall 14, 13.30-15.00, Poster section)

Report 65: Piezoelectric properties of $\text{SrBi}_2(\text{Ta}_x\text{Nb}_{1-x})_2\text{O}_9$ thin films synthesized by the sol-gel method

(WEDNESDAY 20 October, Hall 15, 13.30-15.00, Poster section)

Report 67: Two-steps formation of ZnO-loaded TiO_2 nanotube array films with enhanced photocatalytic performance

(WEDNESDAY 20 October, Hall 3, 11.00-13.00)

Semchenko I.

Report 48: Modeling a three-spike absorber in the range 9-13 GHz (THURSDAY 21 October, Hall 1, 10.00-13.00)

Report 49: Production and experimental study of a weakly reflecting absorbing metamaterial based on planar spirals in the microwave range

(THURSDAY 21 October, Hall 1, 10.00-13.00)

Serdyukov A. N.

Report 51: Simulation of laser splitting of bilayer structures made of silicon wafers and glass substrates (THURSDAY 21 October, Hall 3, 10.00-13.00)

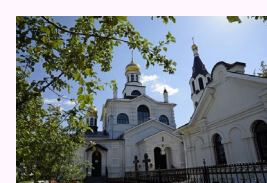
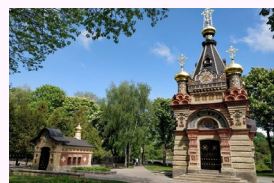
Report 52: The use of artificial neural networks for determining the parameters of laser processing of fused quartz (THURSDAY 21 October, Hall 3, 10.00-13.00)

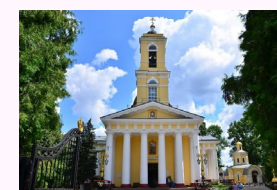
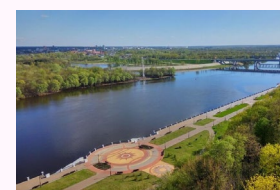
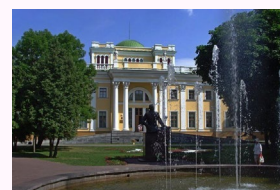
Sereda A. A.

Report 22: The use of design automation tools in training young specialists in radio electronics (THURSDAY 21 October, Hall 3, 10.00-13.00)

Shainidze J. J.

Report 14: 3D Fluorescence spectroscopy of liquid media via internal reference method (THURSDAY 21 October, Hall 2, 10.00-13.00)





Shalini V.

Report 38: Enhancing the seebeck coefficient of Zn-doped MoS₂ grown over carbon fabrics via band engineering
 (WEDNESDAY 20 October, Hall 11, 13.30-15.00, poster section)

Shalupaev S. V.

Report 22: The use of design automation tools in training young specialists in radio electronics (THURSDAY 21 October, Hall 3, 10.00-13.00)

Shamyna A. A.

Report 79: Analysis of the spatial distribution of the second-harmonic radiation generated in a thin surface layer of a spheroidal dielectric particle
 (FRIDAY 22 October, Hall 1, 10.00-12.00)
Report 80: Maxima of the power density of the second-harmonic generation from a linear structure of long cylindrical dielectric particles
 (FRIDAY 22 October, Hall 1, 10.00-12.00)

Sharma P.

Report 16: High-performance and low-voltage current sense-amplifier using GAA-CNTFET with different chirality and channel
 (THURSDAY 21 October, Hall 5, 13.30-15.00, poster section)

Shepelina A. Yu.

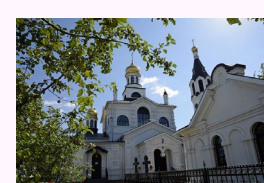
Report 65: Piezoelectric properties of SrBi₂(Ta_xNb_{1-x})₂O₉ thin films synthesized by the sol-gel method
 (WEDNESDAY 20 October, Hall 15, 13.30-15.00, Poster section)

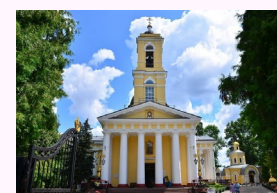
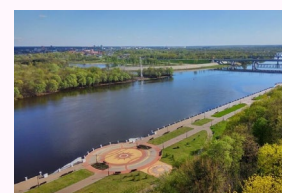
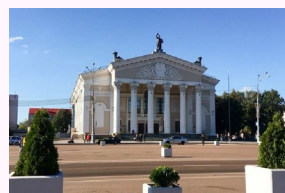
Shershnev E. B.

Report 53: Optimization of quartz glass laser polishing parameters using the computational experiment planning method
 (THURSDAY 21 October, Hall 3, 10.00-13.00)

Shimizu K.

Report 71: The physicochemical/electrical properties of plasma activated medium by dielectric barrier discharge microplasma
 (WEDNESDAY 20 October, Hall 3, 11.00-13.00)





Shimomura M.

[Report 39:](#) Effect of Ag substitution on enhancing the thermoelectric performance of nanostructured SnSe (THURSDAY 21 October, Hall 1, 10.00-13.00)

Shizuka H.

[Report 23:](#) Effects of process parameters on the dissimilar friction stir welded joints between aluminum alloy and polycarbonate
(WEDNESDAY 20 October, Hall 6, 13.30-15.00, poster section)

Shubbar M.

[Report 11:](#) An angle-sensitive, nickel bolometer-based, adaptive infrared pixel antenna (THURSDAY 21 October, Hall 2, 10.00-13.00)

Shumskaya A. E.

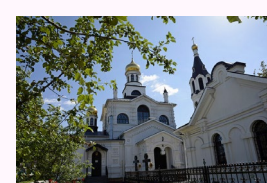
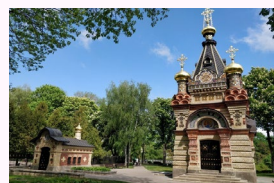
[Report 30:](#) Polyaniline-based food quality markers (WEDNESDAY 20 October, Hall 1, 11.00-13.00)

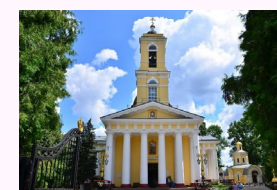
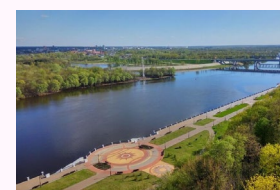
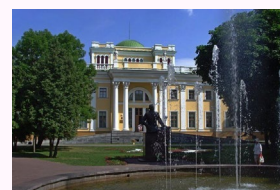
Shvidkiy S.

[Report 3:](#) The proton beam influence on the sensitivity of wheat plantlets to AgNP pollution-preliminary results (WEDNESDAY 20 October, Hall 2, 11.00-13.00)

Sidharth D.

[Report 39:](#) Effect of Ag substitution on enhancing the thermoelectric performance of nanostructured SnSe (THURSDAY 21 October, Hall 1, 10.00-13.00)





Sidski V. V.

Report 32: Synthesis of scintillating glass materials containing yttrium niobate crystallites activated with terbium ions

(WEDNESDAY 20 October, Hall 1, 11.00-13.00)

Report 41: Characteristics of nanocomposite sol-gel films on black silicon surface (THURSDAY 21 October, Hall 11, 13.30-15.00, poster section)

Report 42: AFM topography of $\text{ZnO}_x\text{:MgO}$ nanocomposite sol-gel films on the surface of silicon (THURSDAY 21 October, Hall 12, 13.30-15.00, poster section)

Report 43: Sol-gel synthesis TiO_2 nanotubes based on ZnO nanorods, for use in solar cells (THURSDAY 21 October, Hall 1, 10.00-13.00)

Report 64: Raman investigation of multiferroic BiFeO_3 and $\text{Bi}_{1-x}\text{Sm}_x\text{FeO}_3$ materials synthesized by the sol-gel method

(WEDNESDAY 20 October, Hall 14, 13.30-15.00, Poster section)

Report 65: Piezoelectric properties of $\text{SrBi}_2(\text{Ta}_x\text{Nb}_{1-x})_2\text{O}_9$ thin films synthesized by the sol-gel method

(WEDNESDAY 20 October, Hall 15, 13.30-15.00, Poster section)

Singh Rohitkumar
Shailendra

Report 16: High-performance and low-voltage current sense-amplifier using GAA-CNTFET with different chirality and channel

(THURSDAY 21 October, Hall 5, 13.30-15.00, poster section)

Sirghi L.

Report 62: Atomic force spectroscopy experiments with amino-functionalized silicon AFM tips and samples

(WEDNESDAY 20 October, Hall 13, 13.30-15.00, poster section)

Report 68: Atomic force microscopy indentation of supported lipid bilayers

(WEDNESDAY 20 October, Hall 16, 13.30-15.00, Poster section)

Slepiankou D.

Report 48: Modeling a three-spike absorber in the range 9-13 GHz (THURSDAY 21 October, Hall 1, 10.00-13.00)

Sokolov S. I.

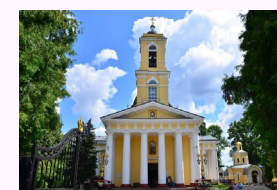
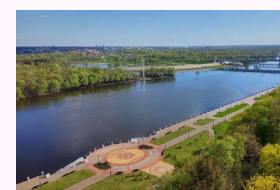
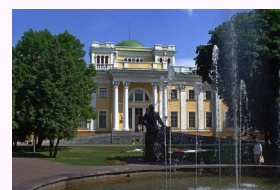
Report 53: Optimization of quartz glass laser polishing parameters using the computational experiment planning method

(THURSDAY 21 October, Hall 3, 10.00-13.00)

Soroka S.A.

Report 42: AFM topography of $\text{ZnO}_x\text{:MgO}$ nanocomposite sol-gel films on the surface of silicon (THURSDAY 21 October, Hall 12, 13.30-15.00, poster section)





Stoian G.

Report 66: Photocatalytic activity and wettability of TiO_2 nanotube arrays coupled with WO_3 and ZnO (WEDNESDAY 20 October, Hall 3, 11.00-13.00)

Sychov M. M.

Report 25: One-step microwave synthesis of Eu^{2+} -doped silicate and chlorinesilicate phosphors mixture for application in light sources (WEDNESDAY 20 October, Hall 1, 11.00-13.00)

Report 28: Digital materials science (WEDNESDAY 20 October, Hall 1, 11.00-13.00)

Report 33: Isotropy mechanical properties products with geometry triple periodic minimal surfaces (TPMS) (THURSDAY 21 October, Hall 1, 10.00-13.00)

Report 36: Impact of modeling method on geometry and mechanical properties of samples with TPMS structure (THURSDAY 21 October, Hall 1, 10.00-13.00)

Report 56: Development of material for 3D printing based on thermoplastic elastomer (THURSDAY 21 October, Hall 3, 10.00-13.00)

Sysoev E. I.

Report 55: Investigation of acoustic wave propagation in complex geometry (THURSDAY 21 October, Hall 3, 10.00-13.00)

Tabata K.

Report 21: Applications for effective representation of imaging with X-ray CT (THURSDAY 21 October, Hall 9, 13.30-15.00, poster section)

Report 75: Spatial resolution of X-ray imaging using $80\mu\text{m}$ pitch TlBr detector (FRIDAY 22 October, Hall 1, 10.00-12.00)

Tabe M.

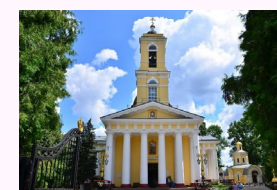
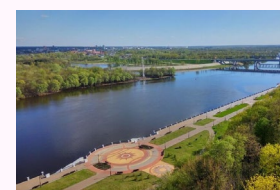
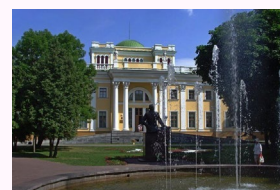
Report 15: First-principles study of bandgap electronic states under electric field in silicon nanowires with discrete dopants (THURSDAY 21 October, Hall 4, 13.30-15.00, poster section)

Report 17: Theoretical study of the impact of a donor-acceptor pair on tunneling current in Si nanodiodes (THURSDAY 21 October, Hall 6, 13.30-15.00, poster section)

Tabrizchi H.

Report 20: Deep learning applications for COVID-19: a brief review (THURSDAY 21 October, Hall 8, 13.30-15.00, poster section)





Takagi K.

[Report 21:](#) Applications for effective representation of imaging with X-ray CT (THURSDAY 21 October, Hall 9, 13.30-15.00, poster section)
[Report 75:](#) Spatial resolution of X-ray imaging using 80 μ m pitch TlBr detector (FRIDAY 22 October, Hall 1, 10.00-12.00)

Takagi T.

[Report 75:](#) Spatial resolution of X-ray imaging using 80 μ m pitch TlBr detector (FRIDAY 22 October, Hall 1, 10.00-12.00)

Takeya K.

[Report 70:](#) High power terahertz wave emission using DAST crystal (WEDNESDAY 20 October, Hall 17, 13.30-15.00, Poster section)
[Report 74:](#) Diamond radiation detector with built-in boron-doped neutron converter layer (FRIDAY 22 October, Hall 1, 10.00-12.00)

Talkachov A. I.

[Report 79:](#) Analysis of the spatial distribution of the second-harmonic radiation generated in a thin surface layer of a spheroidal dielectric particle (FRIDAY 22 October, Hall 1, 10.00-12.00)
[Report 80:](#) Maxima of the power density of the second-harmonic generation from a linear structure of long cylindrical dielectric particles (FRIDAY 22 October, Hall 1, 10.00-12.00)

Tamura Y.

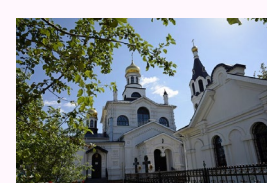
[Report 9:](#) Probing of deep states by band-to-band tunneling in nanoscale silicon-on-insulator Esaki diodes (THURSDAY 21 October, Hall 2, 10.00-13.00)

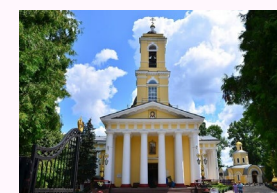
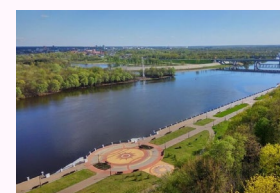
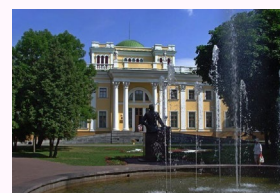
Tanaka Y.

[Report 37:](#) Mechanism of double-step conversion reaction in nanostructured tungsten trioxide anode for Li-Ion batteries (THURSDAY 21 October, Hall 1, 10.00-13.00)

Teodoroff-Onesim S.

[Report 68:](#) Atomic force microscopy indentation of supported lipid bilayers (WEDNESDAY 20 October, Hall 16, 13.30-15.00, Poster section)





Terao T.

[Report 75:](#) Spatial resolution of X-ray imaging using 80 μ m pitch TlBr detector (FRIDAY 22 October, Hall 1, 10.00-12.00)

Tifui G.

[Report 68:](#) Atomic force microscopy indentation of supported lipid bilayers (WEDNESDAY 20 October, Hall 16, 13.30-15.00, Poster section)

Timoshenko M. V.

[Report 56:](#) Development of material for 3D printing based on thermoplastic elastomer (THURSDAY 21 October, Hall 3, 10.00-13.00)

Tkachenko V. I.

[Report 26:](#) Investigation of the convection effect on the inclusion motion in thermally stressed crystals
(WEDNESDAY 20 October, Hall 8, 13.30-15.00, poster section)

Tkachenko V. V.

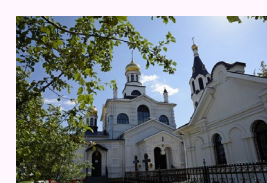
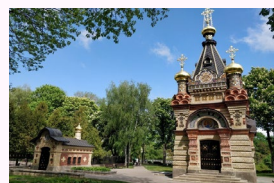
[Report 32:](#) Synthesis of scintillating glass materials containing yttrium niobate crystallites activated with terbium ions
(WEDNESDAY 20 October, Hall 1, 11.00-13.00)

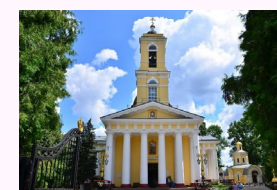
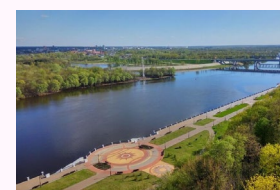
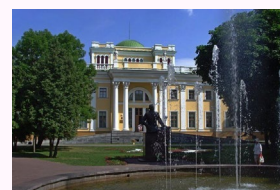
Topala I.

[Report 73:](#) Oxidation and stability of polymers treated by atmospheric-pressure plasma (WEDNESDAY 20 October, Hall 3, 11.00-13.00)

Tóth T. J.

[Report 18:](#) Intelligent pantry: a low cost smart storage manager for food spoilage prevention (THURSDAY 21 October, Hall 3, 10.00-13.00)





Toyoda K.

[Report 75:](#) Spatial resolution of X-ray imaging using 80μm pitch TlBr detector (FRIDAY 22 October, Hall 1, 10.00-12.00)

Tripathi S. R.

[Report 7:](#) In vivo measurement of dielectric properties of human skin using attenuated total reflection terahertz time domain spectroscopy (WEDNESDAY 20 October, Hall 2, 11.00-13.00)

[Report 70:](#) High power terahertz wave emission using DAST crystal (WEDNESDAY 20 October, Hall 17, 13.30-15.00, Poster section)

Tsebriienko T.

[Report 64:](#) Raman investigation of multiferroic BiFeO₃ and Bi_{1-x}Sm_xFeO₃ materials synthesized by the sol-gel method (WEDNESDAY 20 October, Hall 14, 13.30-15.00, Poster section)

Tuchkovskii A. K.

[Report 44:](#) NiO and NiO:Al films for solar cells: a compromise between electrical conductivity and transparency (THURSDAY 21 October, Hall 13, 13.30-15.00, poster section)

Tusor B.

[Report 18:](#) Intelligent pantry: a low cost smart storage manager for food spoilage prevention (THURSDAY 21 October, Hall 3, 10.00-13.00)

Tyulenкова O. I.

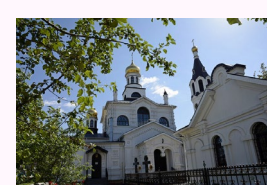
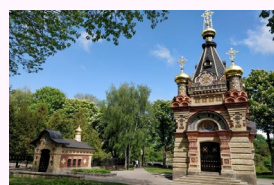
[Report 41:](#) Characteristics of nanocomposite sol-gel films on black silicon surface (THURSDAY 21 October, Hall 11, 13.30-15.00, poster section)

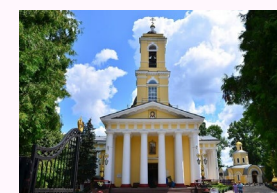
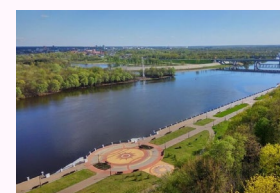
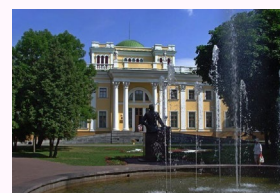
[Report 42:](#) AFM topography of ZnO_x:MgO nanocomposite sol-gel films on the surface of silicon (THURSDAY 21 October, Hall 12, 13.30-15.00, poster section)

[Report 43:](#) Sol-gel synthesis TiO₂ nanotubes based on ZnO nanorods, for use in solar cells (THURSDAY 21 October, Hall 1, 10.00-13.00)

[Report 46:](#) Development of sapphire-like glass by sol-gel technology (THURSDAY 21 October, Hall 1, 10.00-13.00)

[Report 65:](#) Piezoelectric properties of SrBi₂(Ta_xNb_{1-x})₂O₉ thin films synthesized by the sol-gel method (WEDNESDAY 20 October, Hall 15, 13.30-15.00, Poster section)





Uchida H.

Report 70: High power terahertz wave emission using DAST crystal (WEDNESDAY 20 October, Hall 17, 13.30-15.00, Poster section)

Uesugi K.

Report 45: The effect of SiO₂ content rate in simulated lunar regolith on ablation plume temperature and the feasibility assessment of Al₂O₃ reduction (THURSDAY 21 October, Hall 14, 13.30-15.00, poster section)

Várkonyi Kóczy A. R.

Report 1: Investigating urban sustainability by emphasizing on the approaches for reducing fuel consumption using intelligent transportation system (WEDNESDAY 20 October, Hall 2, 11.00-13.00)

Report 2: Environmental risk management by achieving sustainable development goals in architecture and urban engineering (WEDNESDAY 20 October, Hall 2, 11.00-13.00)

Report 18: Intelligent pantry: a low cost smart storage manager for food spoilage prevention (THURSDAY 21 October, Hall 3, 10.00-13.00)

Report 20: Deep learning applications for COVID-19: a brief review (THURSDAY 21 October, Hall 8, 13.30-15.00, poster section)

Report 58: Modeling and optimization of a microgrid for a midrise apartment and industry (THURSDAY 21 October, Hall 3, 10.00-13.00)

Vaskevich V. V.

Report 32: Synthesis of scintillating glass materials containing yttrium niobate crystallites activated with terbium ions (WEDNESDAY 20 October, Hall 1, 11.00-13.00)

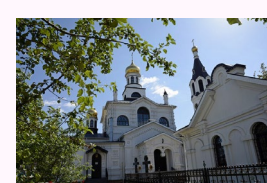
Report 43: Sol-gel synthesis TiO₂ nanotubes based on ZnO nanorods, for use in solar cells (THURSDAY 21 October, Hall 1, 10.00-13.00)

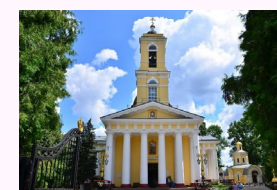
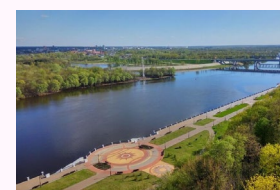
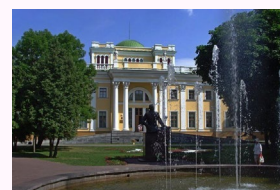
Report 44: NiO and NiO:Al films for solar cells: a compromise between electrical conductivity and transparency (THURSDAY 21 October, Hall 13, 13.30-15.00, poster section)

Report 46: Development of sapphire-like glass by sol-gel technology (THURSDAY 21 October, Hall 1, 10.00-13.00)

Vynohradova-Anik O.

Report 8: Analysis of color coordinates in dried blood spots under aging for forensic medical applications (WEDNESDAY 20 October, Hall 2, 11.00-13.00)





Wibisono G.

[Report 61:](#) Localized surface plasmon resonance liquid sensors based on array gold nanoparticles fabricated on 36XY-LiTaO₃ substrate
(WEDNESDAY 20 October, Hall 12, 13.30-15.00, Poster section)

Xiaohong Jiang

[Report 31:](#) Vacuum coatings based on miramistin and their biological properties (WEDNESDAY 20 October, Hall 1, 11.00-13.00)
[Report 69:](#) Studies of magnesium – hydroxyapatite micro/nano film for drug sustained release (WEDNESDAY 20 October, Hall 3, 11.00-13.00)

Yahaya A. G.

[Report 71:](#) The physicochemical/electrical properties of plasma activated medium by dielectric barrier discharge microplasma
(WEDNESDAY 20 October, Hall 3, 11.00-13.00)

Yamada T.

[Report 74:](#) Diamond radiation detector with built-in boron-doped neutron converter layer (FRIDAY 22 October, Hall 1, 10.00-12.00)

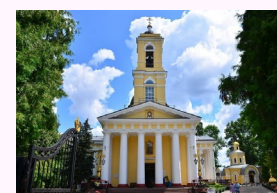
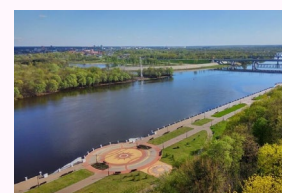
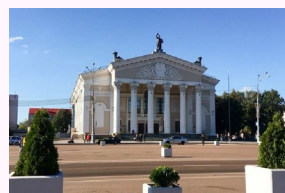
Yamada R.

[Report 12:](#) Evaluation of radiation detection characteristics by α -Ga₂O₃ (THURSDAY 21 October, Hall 2, 10.00-13.00)

Yamaguchi K.

[Report 9:](#) Probing of deep states by band-to-band tunneling in nanoscale silicon-on-insulator Esaki diodes (THURSDAY 21 October, Hall 2, 10.00-13.00)
[Report 15:](#) First-principles study of bandgap electronic states under electric field in silicon nanowires with discrete dopants
(THURSDAY 21 October, Hall 4, 13.30-15.00, poster section)
[Report 17:](#) Theoretical study of the impact of a donor-acceptor pair on tunneling current in Si nanodiodes
(THURSDAY 21 October, Hall 6, 13.30-15.00, poster section)





Yamaguchi T.

Report 12: Evaluation of radiation detection characteristics by α -Ga₂O₃ (THURSDAY 21 October, Hall 2, 10.00-13.00)

Yaremkevych A.

Report 64: Raman investigation of multiferroic BiFeO₃ and Bi_{1-x}Sm_xFeO₃ materials synthesized by the sol-gel method
(WEDNESDAY 20 October, Hall 14, 13.30-15.00, Poster section)

Yarmolenko M. A.

Report 31: Vacuum coatings based on miramistin and their biological properties (WEDNESDAY 20 October, Hall 1, 11.00-13.00)

Yiming Liu

Report 31: Vacuum coatings based on miramistin and their biological properties (WEDNESDAY 20 October, Hall 1, 11.00-13.00)

Zalessky V. B.

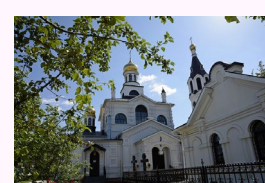
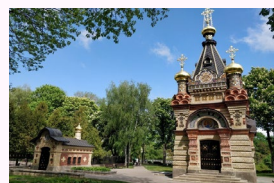
Report 32: Synthesis of scintillating glass materials containing yttrium niobate crystallites activated with terbium ions
(WEDNESDAY 20 October, Hall 1, 11.00-13.00)

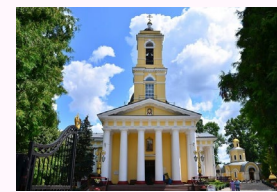
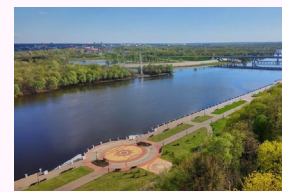
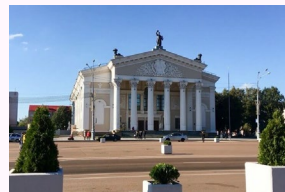
Zelenska K.

Report 8: Analysis of color coordinates in dried blood spots under aging for forensic medical applications (WEDNESDAY 20 October, Hall 2, 11.00-13.00)

Zelenska T.

Report 8: Analysis of color coordinates in dried blood spots under aging for forensic medical applications (WEDNESDAY 20 October, Hall 2, 11.00-13.00)





Zhidko T. V.

Report 30: Polyaniline-based food quality markers (WEDNESDAY 20 October, Hall 1, 11.00-13.00)

